國立交通大學

資訊學院　資訊學程

碩 士 論 文

手控標靶注射與輸注(TCMII) ---

propofol 藥物動力指引系統的

實作性與可行性的初步評估

Target-Controlled Manual Injection and Infusion (TCMII) –

The Implimentation and Preliminary Feasibility Evaluation of a Propofol Pharmacokinetic Guider

研 究 生：吳弘山

指導教授：蕭子健 教授

中 華 民 國 一 百 零 一 年 七 月

手控標靶注射與輸注(TCMII) ---
propofol 藥物動力指引系統的
實作性與可行性的初步評估

Target-Controlled Manual Injection and Infusion (TCMII) – The Implimentation and Preliminary Feasibility Evaluation of a Propofol Pharmacokinetic Guider

研 究 生：吳弘山　　Student: Hung-Shan Wu
指導教授：蕭子健　　Advisor: Tzu-Chien Hsiao

國 立 交 通 大 學
資訊學院 資訊學程

碩 士 論 文

A Thesis
Submitted to College of Computer Science
National Chiao Tung University
in Partial Fulfillment of the Requirements
for the Degree of
Master of Science
in
Computer Science
July 2012

Hsinchu, Taiwan, Republic of China

中 華 民 國 一 百 零 一 年 七 月

手控標靶注射與輸注(TCMII) ---
propofol 藥物動力指引系統的實作性與可行性的初步評估

學生:吳弘山　　指導教授:蕭子健

國 立 交 通大 學　　資 訊 學 院　　資 訊 學 程　　碩 士 班

摘要

目的:到目前為止用群體藥物動力學與藥效學模型控制靜脈麻醉的深度，只能使用 TCI 程控幫浦。不過在麻醉工作中仍常需以手工給藥或用傳統幫浦以 rate control infusion 的方法注射藥劑，因此我們嘗試以藥物動力模型開發手控靜脈注射的 TCMII guider 以協助這方面的工作。由於手控給藥需要考慮長時間的藥物累積效應，需要設計比 TCI 更加有效率的演算法。為了協助人員在手工給藥或設定幫浦流速之前，判斷給藥對作用部位濃度(*Ce*)的影響，此系統首先要能夠快速計算 *Ce* 的走勢，以協助人員判斷與選擇。此外為了降低人員的工作負荷，此系統要能夠即時計算出最佳的注射劑量(OD)與最佳輸注速率(OR)將 *Ce* 維持於目標區(*Cet* range)之內。

研究內容與方法:基於 Schnider 的 propofol 群體藥物動力學模型與藥效學模型，在 Java ME 平台上實作此系統。推算 *Ce* 走勢的方法有三，解析法線性搜尋(ALS)、數值法線性搜尋(NLS)以及實根分離法(RRI)，以 t-test 比較三者所需時間以求其最快者並得知能推算的 *Ce* 走勢有多長久。尋找 OD 與 OR 的方法有二，線性搜尋法與二分搜尋法，也以 t-test 比較二者所需的時間，以求其最快者。再以各種大小的 *Cet* range 與劑量及流速單元量模擬兩小時以上的 target control，以了解使用 TCMII 時所需的人員工作量以初步評估此系統的可行性。

結果:時間範圍愈大，計算 *Ce* 走勢所需的時間愈久。當預測的時間範圍長達 3 小時以上時，RRI 仍能在 0.2 秒內推算 *Ce* 走勢，而 ALS 與 NLS 則否。二分搜尋法能在 1 秒內找出 OD 與 OR，線性搜尋法則僅能找出 OD。如欲將 propofol 的 *Ce* 控制在目標的 90-110% 範圍內，只要每 2 分鐘左右給予一次最佳注射劑量即可。對於同範圍，使用定速幫浦注射，則在穩態之前僅需調整流速為最佳輸注速率 3 次即可。

結論:TCMII 能即時提供 *Ce* 走勢以及 OD 與 OR，以協助麻醉醫師以最少的人員工作量將 *Ce* 控制於 *Cet* range 中。它是目前唯一能將藥物動力模型應用於手控處置靜脈注射以施行 target control 的方法。

Target-Controlled Manual Injection and Infusion (TCMII) – The Implimentation and Priliminary Feasibility Evaluation of a Propofol Pharmacokinetic Guider

Student：Hung-Shan Wu　　Advisor：Tzu-Chien Hsiao

Degree Program of Computer Science
National Chiao Tung University

ABSTRACT

Objective: Population pharmacokinetic/pharmacodynamic (PopPK/PD) models based intra- venous anesthesia need a program-controlled infusion pump so far. But bolus injection or traditional rate control infusion pump is still applied on anesthesia work and that is why a target- controlled manual injection/infusion (TCMII) guider is needed and was developed in this study. Since manual administration has a long term drug accumulation effect, TCMII need a more efficient algorithm to handle effect site concentration (*Ce*) trend. A user has to read *Ce* trend before deciding an injection dose and an infusion rate, so this guider has to plot *Ce* trend timely. Moreover, in order to minimize the human workload, the guider must calculate an optimal injection dose (OD) and an optimal infusion rate (OR) every second to help the user to keep *Ce* in *Cet* range.

Materials and Methods: Based on Schnider's PopPK/PD models of propofol, a TCMII guider was implemented on Java ME platform. T-tests was applied to compare the speed to plot *Ce* trend by analytical linear search (ALS), numerical linear search (NLS) and real root isolation (RRI) methods to find the most efficient one and how long the *Ce* trend can be. The times needed to find out ODs and ORs by linear search (LS) and bisection method (BM) were compared with t-tests to find out which one is faster. The frequencies of using ODs and ORs to keep *Ce* in *Cet* ranges for two or more hours were simulated in order to evaluate the workload of manual target control and the feasibility of this guider.

Results: To plot *Ce* trend on a larger time domain took more time. If time domain size was more than 3 hours, RRI can plot *Ce* trend in 0.2 second but ALS and NLS can not. OD can be searched by BM and by LS in 1 second. But OR can be searched in 1 second only by BM. To keep *Ce* in the range of 90-110% *Cet* needed to inject an OD every 2 minutes. To keep *Ce* in the same range for more than 2 hours needed to set the infusion rate as OR for 3 times.

Conclusion: TCMII can offer users with *Ce* trend and OD and OR on demain. It helps to keep *Ce* in a *Cet* range with minimal and reasonable workload. As we know, it is the only method to apply PK and PD models on target-controlled manual intravenous administrations.

Acknowledgement

I am deeply indebted to my adviser Dr. Tzu-Chien Hsiao whose stimulating, suggestions and encouragement helped me in all the time of research and writing of this thesis. Without his guidance and persistent help this thesis is not possible to been done. Also I would like to thank the professors of College of Computer Science of National Chiao Tung University in helping me to broaden my view and knowledge. As a Co-op student, I am indebted to many of my colleagues in Changhua Christian hospital and Chenchin general hospital, especially Dr. Chou-Lian Chen to support me the off time for my class hours. My colleagues from the LabVIEW team of NCTU supported me in my research work. I want to thank them for all their help, support, interest and valuable hints. I also thank Professor Steven L. Shafer for permission to include his figures and tables in my thesis. I have to express sincere gratitude to Dr Shou-Jen Fan and Dr Yi Chang to audit this thesis strictly and to advise me kindly on my final oral defense examination. Above all, I thank my wife, Lili who stood beside me and encouraged me constantly. Her patient love fully enabled me to complete this work.

Contents

List of Figure Captions

List of Table Captions

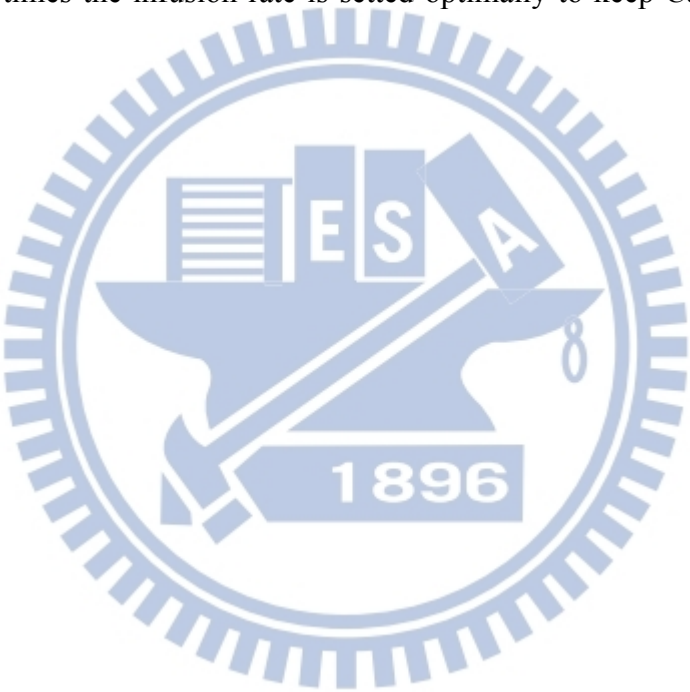

List of Appendices

Notations, Acronyms, Abbreviations and Terms

Notations:

A_i	mass of drug in comparment i, i=1 to 4
c_i	drug concentration in compartment i, i=1 to 4
Ce	effect compartment concentration, $=c_4$
Cet	the target of effect compartment concentration
CL_i	clearance of comparment i, i=1 to 4
Cp	drug concentration of central compartment (blood plasma)
k_{ij}	micro-rate constants. The drug transfer rate from compartment i to compartment j is $k_{ij} \cdot A_i$
LB	lower bound of *Cet* range
n_{sp}	length of of *Ce* sampling point sequence, sampling through time domain
Pu	*Ce* peak value after one unit dose of drug injected to a person who has no drug in the body
Qd	step quantity of injection dose
Qr	step quantity of infusion rate
tc	the time to start an infusion
td	the time to discontinue an infusion
t_0	the time to recalculate optimal injection dose and infusion rate, also be the begining of the time domain of *Ce* trend function
TMax	the maximum of *Ce* trend within its time domain
TMin	the minimum of *Ce* trend within its time domain
t_{peak}	the time from the initial bolus injection to peak *Ce*
UB	the upper bound of *Cet* range
V_i	the volume of the comparment i, i=1 to 4

Acronyms abbreviations and terms listed in alphabetic order:

ALS: analytical linear search

CCIP: computer controlled infusion pump

Cet range: the range of *Cet*, bounded by *LB* and *UB*

Ce trend: the trend of *Ce* following a serial of manual administrations and not to inject drug or

change the infusion rate within the time interval (t_0, t_0+z], where z denotes the size of time domain.

MEF: multi-exponential polynomial

NLS: numerical linear search

Optimal infusion rate, optimal rate: the minimal infusion rate that keeps *Ce* trend from being less than *LB*.

Optimal injection dose, optimal dose: the maximal injection dose that can elevate *Ce* into *Cet* range and do not raise *Ce* over *UB*.

PK: pharmacokinetic

PD: pharmacodynamic

PopPK: population pharacokinetic

RRI: real root isolation with pseudo-derivative sequence and bisection method

TCI: target-controlled infusion

TCMII: target-controlled manual injection and infusion

TIVA: total intravenous anesthesia

Chapter 1: Introduction

1.1. Motivation

In addition to total intravenous general anesthesia [1], intravenous drugs are used in induction of inhalational general anesthesia, muscle relaxation in general anesthesia, sedation and analgesia for invasive procedures like gastroscopy and colonoscopy and post-operative pain management. Intravenous route is the most frequently used route in anesthesia drug administration.

An ideal intravenous anesthetic drug effect should onset quickly, be maintained steadily and recover predictablely [2]. The ultimate goal of a particular dose of drug is to obtain the desired clinical effect, taking into account the interindividual pharmacokinetic and pharmacodynamic variability. Recent findings suggest that effect compartment-controlled target-controlled infusion systems and measurement of clinical drug effects might be helpful to optimize the administration of intravenous anesthetics and opioids [3].

Currently, computer controlled infusion method such as the target-controlled infusion (TCI) is the only way to apply pharmacokinetic models on clinical practice. To control drug effect with TCI is far easier than with manual injection or infusion because the relationship between effect site concentration and drug response does not change over time or change with dosing history [4].

But TCI is not approved by FDA so far and is not clinically available in North America [5]. It depends on special and expensive pumps. And even the mostly used drug, propofol [6], in TCI is still manually used worldwide. There is no technology to apply pharmacokinetic models on manual intravenous injection or infusion before this research.

A pharmacokinetic modeling guider for manual intravenous administrations on a handheld device will enable anesthetists to apply the power of pharmacokinetic models on demand anywhere and anytime.

1.2. Problem discription

Portability is essential to a target-controlled manual injection and infusion (TCMII) guider because manual administration might be executed anytime and everywhere. We try to develop a TCMII guider on a Java ME platform that is supported by most of the handheld devices. The calculation speed of a handheld device is limited so the efficiency of algorithms

to calculate the effect site concentration (*Ce*) trend or to find proper infusion rates and injection doses is important.

In TCI system, the user controls the *Ce* target (*Cet*) and the machine keep *Ce* value very close to *Cet* by frequently adjust the infusion rate. A human user can not do manual administrations as frequently as TCI system. In TCMII guider, since *Ce* is time-variant with manual control, the user controls a *Cet* range in addition to *Cet*. This range is bounded by a lower bound (*LB*) and an upper bound (*UB*) with *Cet* in the middle. *Cet* percentage range is defined as $\frac{UB - Cet}{Cet} \cdot 100\% (= \frac{Cet - LB}{Cet} \cdot 100\%)$.

TCMII guider is designed for two purposes. Firstly, when a user controls injection and infusion, the guider offers the related *Ce* trend. The user input intended injection doses or infusion rates into the guider and read the output *Ce* trend to decide whether to accept it or not. Secondly, when a user controls the *Cet* range, the guider proivides optimal injection doses and infusion rates to help to keep *Ce* in *Cet* range and reminds the user timely. Here, the word "optimal" means to let the user do manual administrations least frequently.

Ce trend must be replied in 0.2 second, as we specified, because a user might click a button up to 5 times to request the guider to forecast *Ce* trend in a second. The first question is that is there any algorithm efficient enough and faster than others?

Ce trend following a serial of manual drug administration is a multi-exponential function [appendix 1-11]. There are two straightforward algorithms to calculate *Ce* values and plot *Ce* trend. They are analytical and numerical linear search methods.

Analytical linear search (ALS) method [appendix 17] calculates *Ce* values analytically. The most time-consuming process that is to get the values of exponential functions limits the efficiency. So a more efficient algorithm, numerical linear search method, is introduced.

Numerical linear search (NLS) method [appendix 18] calculates *Ce* values numerially with Euler's differential equation. Free from exponential function calculation, it is quicker then ALS, but has potential problems like accumulated rounding error and oscillation [7].

If the number of sampling points of *Ce* trend is denoted as n_{sp} then it is the product of the sampling frequency multiplied by the size of *Ce* trend time domain. With a fix sampling frequency, the greater n_{sp} is, to plot whole *Ce* trend needs the more time.

The *Ce* trend time domain of propofol TCI is less than 2 minutes and both linear search

algorithms can calculate *Ce* trend efficiently[7]. But they may not be efficient enough for larger time domain of TCMII guider. A recently developed theoretically more efficient method, real root isolation (RRI) technique, is applied on real-time PK system unprecedentedly.

Real root isolation method, developed to find real roots of multi-exponential polynomial functions by pseudo-deravative sequence [8], is refined to calculate extrema of *Ce* trend which are multi-exponential functions (MEF) [appendix 12-13]. This method transforms a problem of finding real roots of a higher degree MEF into the problem of finding real roots of its pseudo-deravative function that is a lower degree MEF [appendix 12]. Repeat this process until the problem is transformed into finding the real root of a single exponential function and solve it deterministically. This method extracts the information of extrema of *Ce* trend but *Ce* values between extrema are ignored.

The time needed for ALS and NLS to resolve the roots of MEF is $O(n_{sp})$ and for RRI is $O(\lg n_{sp})$. But the algorithm of RRI is much more complex than ALS and NLS, so it is necessary to find out that which one is the most efficient algorithm by simulations.

Other than to forecast *Ce* trend for user's administrations, TCMII guider should offer optimal infusion rates or injection doses and to maintain *Ce*. The first strategy to maintain *Ce* is to inject some drug whenever the whole following *Ce* trend is going to be under the lower bound of *Cet* range. The guider offers optimal injection doses to keep *Ce* in its target range. An optimal injection dose is defined as the maximal injection dose that can elevate *Ce* into *Cet* range without overshooting the upper bound. In figure 1, the *Ce* trend that follows adding 22mg propofol when *Ce* is descending below its lower bound at time 00:02:47 is an example of optimal injection dose effect. Optimal injection dose is the best choice of bolus dosage to drive *Ce* into *Cet* range quickest and stay in the range longest.

The second strategy is to maintain *Ce* with an infusion pump. Inject an optimal dose to elevate *Ce* into the *Cet* range when the whole *Ce* trend is under the range; stop any infusion when the whole trend is beyand the range. When *Ce* is in the range, constant rate infusion keeps it in the range much longer than repeated injections. An optimal infusion rate is defined as the minimal rate to keep *Ce* from below the *Cet* range. Demonstrated in figure 2, a user can keep *Ce* in the range by repeated setting infusion rate optimally when *Ce* is close to the upper bound. To Use optimal injection doses and optimal infusion rates can reduce the frequency of manual administration and can reduce the clincal workload.

The sampling frequency selected for TCMII is 1 Hz like the one selected for TCI [2]. For this reason, the guider should refresh *Ce* value and *Ce* trend per second. As the values of optimal injection dose and optimal infusion rate change unceasingly, the guider must present new values every second. Two questions need to be answered. Is it possible to search for an optimal injection dose and an optimal infusion rate in one second?

There are two candidate algorithms to search optiaml injection dose and optimal infusion rate, linear search and bisection method search. The former is based on the definitions of optimal injection dose and optimal infusion rate. The latter is based on the correlation between injection dose and the maximum of *Ce* trend (*TMax*) [appendix 14] and the correlation between the infusion rate and the minimum of *Ce* trend (*TMin*) [appendix 15].

If optimal injection doses and infusion rates can be found timely, two more questions arise. Is the workload of both strategies feasible for human staff? We temporarily assume that if the frequency of injecting optimal doses to keep *Ce* in *Cet* range is less than once per two minutes then the first strategy is reported as feasible. And if the frequencies of setting infusion pump at optimal rates to keep *Ce* in *Cet* range is less than once every 10 minutes then the strategy is reported feasible. These assumptions need further clinical evaluations but they are beyond the scope of this thesis.

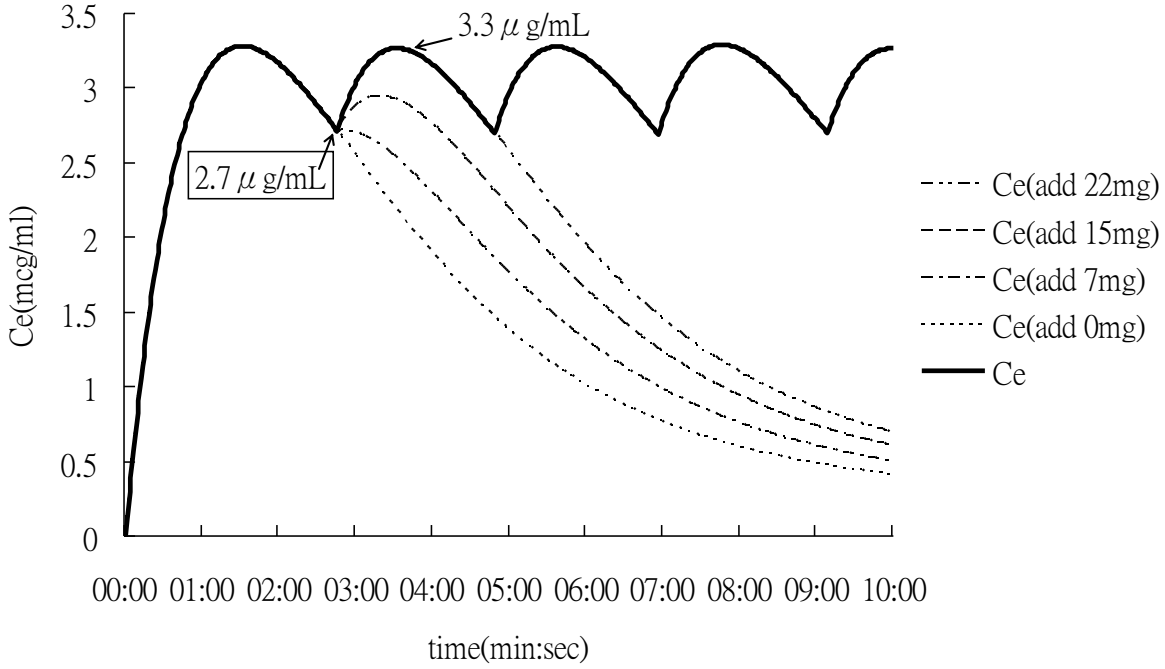

Figure 1. An example of optimal injection dose. The lower bound of *Cet* range is 2.7mcg/mL. When *Ce* is getting lower than the lower bound of *Cet* range, an injection dose is needed. The higher the injection dose is, the higher the following peak value of *Ce* is. An optimal dose is the dose that produces the highest peak value without overshoot the upper bound of *Cet* range (3.3 mcg/mL in this case). Repeatedly inject

optimal dose can keep *Ce* in *Cet* range with least workload.

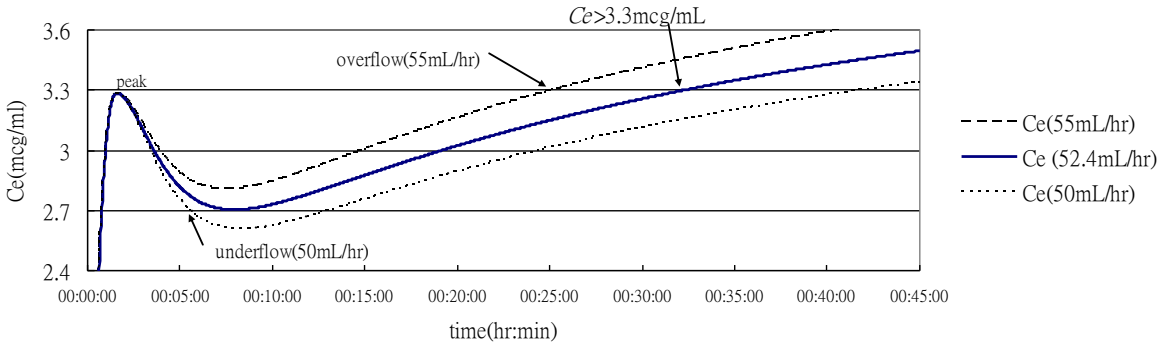

Figure 2. **An example of optimal infusion rate.** An initial loading injection dose was given at the time 00:00:00 and produced a *Ce* peak value near the upper bound of *Cet* range (3.3 mcg/mL). Three infusion rates (50, 52.4, 55 mL/hr) began at the time of *Ce* peak and the related 3 sets of *Ce* trend were plotted. The *Ce* trend of the optimal rate (52.4 mL/hr) concaves above the lower bound of *Ce* target range (2.7mcg/mL) and was kept in the range longer than other rates. When *Ce* is going to rise beyond the upper bound, a new optimal infusion rate shall be setted. To use optimal rates repeatedly keeps *Ce* in *Cet* range and costs the least workload.

Chapter 2: Literature review

Drug concentration control is crucial in routine patient care when there is significant consequence associated with therapeutic failure or toxicity, wide interpatient pharacokinetic variability, narrow therapeutic range, and the demonstrated utility of drug concentration monitoring as an intermediate end point to guide therapeutic decisions. However, it is not yet consistently available in all clinical settings in which there is a need [9].

Constant rate infusion pumps were designed to administer a wide range of infusion rates as well as a bolus dose. However, it is difficult to maintain optimal anesthetic conditions to titrate a drug according to the changing needs of the patient [10]. One of the resolutions is to apply pharmacokinetic model on open-loop or close-loop control of regimen.

2.1. Pharmacokinetics

Pharmacokinetics studies on the way the body deals with absorption, distribution, metabolism, and excretion of drugs under investigation expressed in mathematical terms [11]. Applied pharmacokinetics is a challenging clinical discipline with a strong theoretical framework for impoving patient outcomes by controlling for variability in drug disposition among individuals [10].

Pharmacokinetic analysis is performed by noncompartmental (model independent) or compartmental methods. Compartmental pharmacokinetic analysis uses pharmacokinetic models to describe and predict the concentration-time curve. The main advantage of compartmental methods over noncompartmental methods is the ability to predict the concentration [11].

Multicompartment modeling requires the adoption of several assumptions, such that systems in physical existence can be modeled mathematically:

1. Instant homogeneous distribution of materials within a compartment;
2. The exchange rate of materials among the compartments is propotional to the densities of these compartments. Such as the transfer rate from compartment i to compartment j is $k_{ij}A_i$, while A_i is the mass of drug in compartment i and k_{ij} is a rate constant;
3. Usually, it is desirable that the materials do not undergo chemical reactions while transmitting among the compartments [12].

In practice the number of compartment is usually limited up to 3, since biological and assay variability do not permit estimation of additional coefficents and exponents from the observed data [2]. The polyexponential disposition function can be mathematically transformed into a multicompartment mammillary model with drug administration into a central compartment and transfer by first-order processes into peripheral compartments [appendix 1].

Once a pharmacokinetic model is selected, it is useful to establish the functional relationships between pharmacokinetic properties and patient charateristics [9]. That is the utility of population pharmacokinetic models.

2.2. Population pharmacokinetics

Population pharmacokinetics is the study of the sources and correlates of variability in drug concentrations among individuals who are the target patient population receiving clinically relevant doses of a drug of interest. The population model defines at least two levels of hierarchy, i.e. the variance of individual pharmacokinetic observations and the probability and distribution of these individual parameters modeled as a function of individual-specific covariates [13]. The pharmacokinetic models and parameters that are being used can be derived from previously performed population pharmacokinetic studies [10, 14].

Nonlinear mixed-effect modeling is a commonly used population-based modeling approach. It can estimate intraindividual and interindividual variability. It can limit the influence of outlying samples and individuals through the use of Bayesian statistical analysis, and can provide a potential means of optimizing drug delivery regimens, especially defining pharmacokinetic-dynamic models for target-controlled infusion systems [15].

2.3. Computer-controlled infusion based on the PK model derived from PopPK

In 1968, Kruger-Thiemer first proposed a two-compartment model to achieve and maintain the steady state of blood drug concentration [10, 16]. The results demonstrated that a loading dose was necessary to fill up the initial volume of distribution in order to achieve steady state. In 1981, Schwilden proposed a method to maintain a constant drug concentration of central compartment (c_1) in a three-compartment model [2]. Give a loading bolus injection dose($=c_1 \cdot V_1$) to achieve that concentration instantaneously and give a time varing infusion

rate to keep c_1 constant (figure 3).

Software for systems such as Stanpump (Stanford), Stelpump (Stellenbosch) and Rugloop have been made available since 1990. Initially, the different groups used different terminologies to describe their systems such as CATIA, TIAC, CACI and CCIP. Finally, target controlled infusion (TCI) was the term used to globally describe all these systems [10].

Schnider's population pharmacokinetic model of propofol is one of the most popular clinical applied models on target controlled infusion systems. The derived pharmacokinetic models are three-compartment mammillary models with one central compartment (compartment 1) and two peripheral compartments (compartment 2 and 3). The pharmaco-kinetic parameters including the distribution volumes of compartments (V_1, V_2 and V_3), the metabolic clearance (CL_1), the clearances between central and two peripheral compartments (CL_2 and CL_3) are expressed as functions of age, weight, height and lean body mass [17]. In appendix 1 to appendix 6, the drug concentration of central compartment is derived from these parameters.

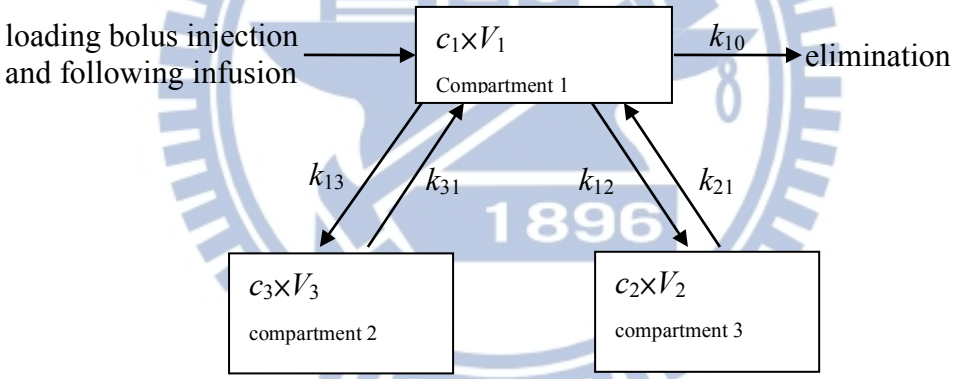

Figure 3. **Schwilden's method to maintain a constant drug concentration of compartment 1 in a three-compartment model**

1. c_i: drug concentration of compartment i
2. V_i: distribution volume of compartment i
3. k_{ij}: The drug mass moves from compartment i to j at the rate of $k_{ij}c_iV_i$, for i=1 to 3.
4. k_{10}: The drug mass is eliminated from compartment 1 at the rate of $k_{10}c_1V_1$.
5. Loading bolus injection dose is c_1V_1 and is given at the begining. Let t be time and c_1 is kept constant by an infusion rate function, $I(t)$.
6. The drug accumulation rate of compartment 2 is $\frac{d(c_2V_2)}{dt} = k_{12}c_1V_1 - k_{21}c_2V_2$. Since c_1 is kept constant and the initial value of c_2 is 0, the drug accumulation rate of compartment 2 is $c_1V_1 \cdot k_{12}e^{-k_{21}t}$. For the same reason the drug accumulation rate of compartment 3 is $c_1V_1 \cdot k_{13}e^{-k_{31}t}$.
7. The infusion rate function to keep c_1 constant is $I(t) = c_1V_1\left(k_{10} + k_{12}e^{-k_{21}t} + k_{13}e^{-k_{31}t}\right)$.

2.4. PK-PD model with an effect compartment

Physically the central compartment (compartment 1) represents blood plasm, and the drug concentration in compartment 1 (c_1) represent the drug concentration of blood plasma ($Cp=c_1$). It should be noted that c_1 do not necessarily reflect drug concentration (or amount) at the site of drug effect at all times after administration [9]. Maintenance of a steady blood plasma drug concentration is not rational when the clinical goal is to rapidly achieve and maintain a steady level of drug effect that is supposed to be related to the drug concentration of effect site (*Ce*) [2]. However the absolute concentration in the effect site cannot be known, because it is the concentration in the immediate milieu of the receptor that cannot be sampled in the intact animal [2].

As independently proposed by Hull et al. [18] and Sheiner et al. [19], the site of drug effect can often be modeled as compartment 4, the "effect site" or effect compartment, whose volume is V_4, and the drug concentration in it is c_4. The compartment 4 is connected to the compartment 1 by a first-order transfer process, as the other peripheral comparmtments. Shafer et al. proposed a more symmetric four-compartment model and define the micro-rate constants of drug transfer rate between compartment 1 and compartment 4 are k_{14} and k_{41} [appendix 7]. The compartment 4 is defined very small to have negligible influence on drug accumulation of compartment 1 to 3 [2]. The pharmacokinetic parameters between compartment 1, 2 and 3 and metabolic clearance are the same with the related three-compartment model and the drug disposition functions of compartment 1, 2 and 3 are the same to the related three-compartment model, too.

Since the effect of drug is related to the drug concentration of effect compartment ($Ce=c_4$), these models with effect compartment link pharmacokinetic and pharmacodynamic informations.

Ignoring the arterio-venous circulation and mixing times, administration of a bolus produces an immediate peak in *Cp* and a subsequent peak in *Ce*. Because the system is linear, when no drug is initially present in the body, the height of the peak *Ce* is proportional to the administered dose, and the peak occurs at the same time, regardless of the dose of the bolus injection (figure 4).

The value of mearsured t_{peak}, defined as the time from inject drug when no drug is present in the body to peak *Ce*, is decided by k_{14} in a four-compartment model. In STANPUMP, a computer controlled infusion system developed by Shafer et al., they reversely use t_{peak} to infer the value of k_{14}. With a very small V_4 and the inferred k_{14}, *Ce* is

derivable and controllable at all times. Targeting on *Cp* makes an implicit assumption that the equilibration between the blood plasma and the effect site is instantaneous ($k_{14}=\infty$) but that's scarcely true. Even a poor estimate of k_{14} may well be closer to providing the desired therapeutic effect than the assumption of instantaneous equilibration between the blood plasma and the effect site [2].

The use of a target controlled infusion device, delivering proportional changes based on pharmacokinetic principles, allows titration of the concentration against clinical effect in individual patients. The titration is based on the concentration–response relationship instead of the dose-response or infusion rate-response relationship [20].

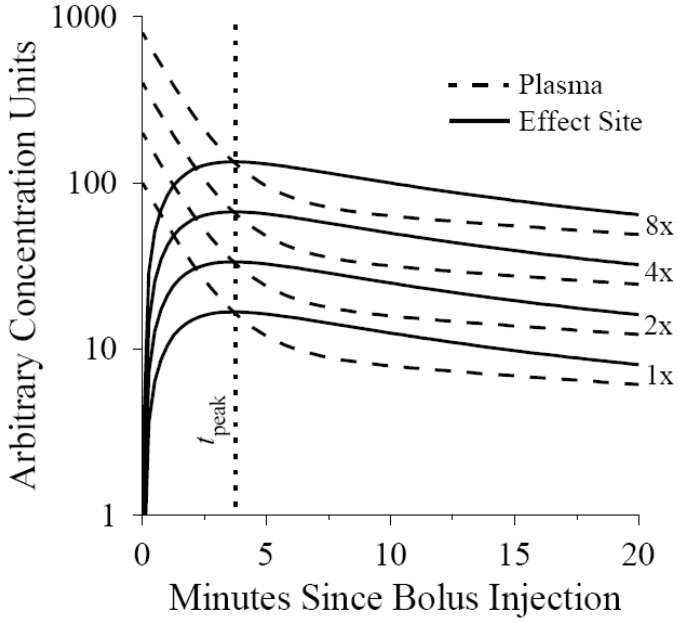

Figure 4. **The t_{peak} is independent of initial bolus dose.** When no drug is present in the body, the peak effect site concentration following a bolus of drug is proportional to the dose, while the time to peak effect site concentration (t_{peak}) is independent of dose [2].

2.5. Computer-controlled infusion based on PK-PD model

TCI system, affording the control technology of derived *Ce* has been developed as a standardised infusion system for the administration of opioids, propofol and other anesthetics by target controlled infusion. The technique of TCI strongly influences the development of intravenous anesthesia and opens a scenario of new and exciting applications in peri-operative anesthetic management [21].

Intermittent injections can result in continuous, rapid fluctuations in concentration. The adventages of computer-controlled infusion over intermittent injections are 1) a lower incidence of responsiveness, 2) greater hemodynamic stability, 3) no patients requiring antidote postoperatively, and 4) an incidence of side effects that tended to be lower [22].

The algorithm proposed by Shafer et al. [2] to control the *Ce* by controlling infusion rate has to adjust infusion rate frequently. The algorithm is summerized to the following steps:

1. Calculate a *Ce* value sequence **A**, (sampling at 1Hz from 0 to 10+t_{peak} sec) of a 10-second infusion (rate = 1 unit/sec, begin from 0 and stop at 10 sec) administered to a PK model without any previously given drug.
2. Every 10 seconds, the TCI system sets infusion rate to a new constant rate and runs for 10 seconds (rate = **r** unit, from *tc* to *td*, *td* =*tc* + 10 sec). The system must calculate the rate of next 10-second infusion before time *tc*. Calculate a *Ce* value sequence **B**, (sampling at 1Hz from *tc* to *td*+t_{peak} sec) resulting from all of the infusions before *tc*.
3. Multiply each element of sequence **A** by some infusion rate (such as **r** unit), and add to related element of seqence **B** to form a new sequence and find out the maximum from it.
4. Try all candidate **r** and search for the infusion rate that produce a maximal *Ce* that is most close to but not greater than *Cet*. This found rate is the next infusion rate from *tc* to *td*
5. Repeat step 2 to 4 until end of the infusion.

This algorithm stands on the fact found by Shafer that if there is already drug in the body, the time from a bolus to the following *Ce* maxmum is always less than t_{peak}. Since any input can be reduced to an infinite series of infinitesimal boluses, it means that the time from end of a brief infusion to the following *Ce* maximum is always less than t_{peak} , so the *Ce* maximum can be found between *tc* and *td*+t_{peak} [2]. Since t_{peak} is around several minutes the size of sequences are limited to hundreds and the algorithm can find the next infusion rate within 10 seconds, in other words, find proper infusion rates timely.

The algorithm of TCI is effective but can not be applied on manual infusion or on bolus guide because TCI demands frequent adjustment of infusion rate that can not be executed manually. Secondly, the interval of constant rate infusion is uncertain and expected to be as long as possible, maybe several minutes,hours or days in manual control, so the sequence **A** and **B** are too long to be handled in real time.

2.6. Close-loop system

TCI system provides model-based open-loop control for drug delivery and maybe inaccurate in drug administration because of model mismatch between the population model and an individual patient's behaviour. The model discrepancy can be overcome by the use of closed-loop control techniques if there is a reliable feedback signal [23]. In closed-loop systems for drug delivery, the effect of a drug is measured and used to adjust drug administration to achieve actual therapeutic states rather than target drug concentrations [24]. In principle, the use of feedback in closed-loop systems may offset the sources of variability in the processes between drug delivery and drug response, of which the most obvious is the inaccuracy of population pharmacokinetic models as applied to individuals in open-loop TCI systems [25].

Although closed-loop systems are virtually ubiquitous, they are infrequently used in anesthesiology because of the complexity of physiologic systems and the difficulty in obtaining reliable and valid feedback data from the patient [26]. Most of the medical standards strictly require that medical systems should be open loop and only human operator can give final decisions.

2.7. Manual injection and infusion

To rapidly achieve and maintain a constant blood plasma concentration for most intravenous drugs, it must be administered as an initial bolus injection followed by a combination of exponentially declining plus constant-rate infusions. In the clinical practice of anesthesia and critical care medicine this was considered not practical without specialized equipment [27].

During surgical operation, the requirement of drug effect changes violently. The fluctuating *Ce* trend following injections makes it even more difficult to titrate to a proper dose. Computer simulation studies found that a dose larger than needed will achieve *Cet* at an earlier time but will necessarily overshoot the *Cet*. The earlier to achieve *Cet*, the greater will be the overshoot [2, 28].

A 'ten-eight-six' regimen to keep mean whole blood propofol concentration to be 3.24 ~ 4.07 $mg \cdot ml^{-1}$ during infusion is once a popular and widely accepted manual infusion scheme for propofol administration. This regimen can be proportionally adjusted to get a higher or lower level of blood propofol [29]. But the blood propofol concentration is unpredictable if a user tries to change the target concentration during infusion based on clinical requirement.

Potentially, TCI and manually controlled infusion (MCI) can result in similar depth of anesthesia and hemodynamic stability without difference in absolute performance errors when titrated against traditional clinical signs [30]. The North American users mainly use MCI or bolus injection because the U.S. Food and Drug Administration (FDA) for a variety of concerns about computer-based drug delivery [5] do not approve the TCI system.

In this thesis three types of manual administrations were considered. They are fast bolus injection, ceased constant rate infusion run for a while and ongoing constant rate infusion. As addressed in appendix 3 and appendix 8, if a single injected bolus dose, *d*, is given at time *tb* then the *Cp* and *Ce* function are:

$$Cp_{tb}(t) = \sum_{\sigma=1}^{3} d \cdot C_\sigma e^{-\lambda_\sigma (t-tb)} \tag{1}$$

$$Ce_{tb}(t) = \sum_{\sigma=1}^{3} d \cdot \left(\frac{k_{e0} C_\sigma}{k_{e0} - \lambda_\sigma} e^{\lambda_\sigma (t-tb)} \right) - d \cdot \left(\sum_{\sigma=1}^{3} \frac{k_{e0} C_\sigma}{k_{e0} - \lambda_\sigma} \right) e^{\lambda_4 (t-tb)} \tag{2}$$

Appendix 4 and 9 state that an ongoing infusion running at the rate *r* started from time *tc* produces the *Cp* and *Ce* as:

$$Cp_{tc\sim}(t) = -\sum_{\sigma=1}^{3} r \cdot \frac{C_\sigma}{\lambda_\sigma} e^{-\lambda_\sigma (t-tc)} + \frac{r}{V_1 k_{10}} \tag{3}$$

$$Ce_{tc\sim}(t) = -\sum_{\sigma=1}^{4} r \cdot E_\sigma e^{-\lambda_\sigma (t-tc)} + \frac{r}{V_1 k_{10}} \tag{4}$$

Appendix 5 and 10 state that a ceased infusion started from time *tc* and stopped at *td* produces the *Cp* and *Ce* as:

$$Cp_{tc\sim td}(t) = \sum_{\sigma=1}^{3} r \times \frac{C_\sigma}{\lambda_\sigma} \left(-e^{-\lambda_\sigma (t-tc)} + e^{-\lambda_\sigma (t-td)} \right) \tag{5}$$

$$Ce_{tc\sim td}(t) = \sum_{\sigma=1}^{4} r \times E_\sigma \left(-e^{-\lambda_\sigma (t-tc)} + e^{-\lambda_\sigma (t-td)} \right) \tag{6}$$

Linearly combine these equations depicting every injection and infusion produces the *Cp* and *Ce* function following a serial of manual injections and constant rate infusions in the form of:

$$Cp_{ii}(t) = \alpha_0 + \sum_{\sigma=1}^{3} \alpha_\sigma e^{-\lambda_\sigma t} \tag{7}$$

$$Ce_{ii}(t) = \varepsilon_0 + \sum_{\sigma=1}^{4} \varepsilon_\sigma e^{-\lambda_\sigma t} \tag{8}$$

They are described in appendix 6 and 11.

2.8. Analytical linear search & numerical linear search

A multicompartmental model with the first-order rate of exchange between compartments can be tranformed into a series of differential equations. These differential equations can be transformed into first-order difference equations. Euler's numerical technique allows calculation of the appoximate amount of drug in each compartment at each update cycle, and this technique has been used in several computer-controlled infusion pumps [7, 31].

Maitre [32] and Jacobs [33] have published analytical solutions for the triexponential equation but they are not used in current computer-controlled infusion pumps for their mathematical complexity [34]. In this thesis the drug amount of the effect compartment in the four-compartment model is transformed into a tetraexponential equation. To our best knowledge, there is no practical analytical resolution for the tetraexponential equation.

To find the optimal infusion rate and injection dose to drive *Ce* into *Cet* range and maintain it in *Cet* range can be transformed into a problem of finding the maximum and minimum of the tetraexponential equation of *Ce* trend within a specific time interval [appendix 14-15].

2.9. Real root isolation of univariate multi-exponential polynomials

Real root isolation problem is to compute a list of disjoint intervals, each containing a distinct real root and together containing all.

Let $p^*(x) = \sum_{i=0}^{n} p_i(x)\lambda_i^x (0 < \lambda_0 < \lambda_1 < \ldots < \lambda_n \wedge p_i(x) \in \Re[x] \setminus \{0\})$ be a multi-exponential polynomial (MEP). Then the degree of $p^*(x)$ is $n + \sum_{i=0}^{n} \deg(p_i)$ is denoted by $\deg(p^*)$ and the tail base λ_0 is denoted by $\text{tbase}(p^*)$. A pseudo-derivative sequence of p^* can be constructed recursively as follows:

$$\begin{cases} F_0 = \dfrac{p^*}{(\text{tbase}(p^*))^x} \\ F_{i+1} = \dfrac{F_i'}{(\text{tbase}(F_i'))^x} \end{cases} \tag{9}$$

until $\deg(F_{i+1}) = 0$ [8].

Appendix 12-13 shows a simplified version of root isolation theorums and algorithm for multiple-exponential function by way of pseudo-derivative sequence.

2.10. Classification of the control techniques of intravenous administration

The control techniques can be classified by the application of pharacokinetic models or not into non-model-based or model-based ones. The facilities can be classified into none, simple rate control infusion pump, open-loop system that has no physical information feed back, closed-loop system that depend on physical information. Before this thesis, the area of model-based control with or without rate-control infusion pump is undeveloped.

Table 1. **The classification of control techniques of intravenous administration**

	non-model-based	**model-based**
without infusion	manual injection	null
rate control infusion	manual infusion	null
open-loop system	patient control adapter	target-controlled infusion
closed-loop system	Rule-based control [35] PID controller [36]	Sedasys® [37] Fuzzy control [38]

Chapter 3: Materials and methods

3.1. Simulation 1. How long it takes to plot *Ce* trend.

This simulation was designed to answer the first question in section 1.2.: Is there any algorithm to be quick enough to forecast *Ce* trend in 0.2 second? The algorithm to plot *Ce* trend in less than 0.2 second is considered feasible. The candidate algorithms are ALS, NLS and RRI as described in appendix 17-18 and 13. The sampling frequency is 1 Hz.

Every manual administration, either bolus injection or constant rate infusion, produces a specific *Ce* trend [appendix 8-10]. *Ce* trend following a serial of manual administrations is the summation of *Ce* trend produced by every single administration [appendix 11].

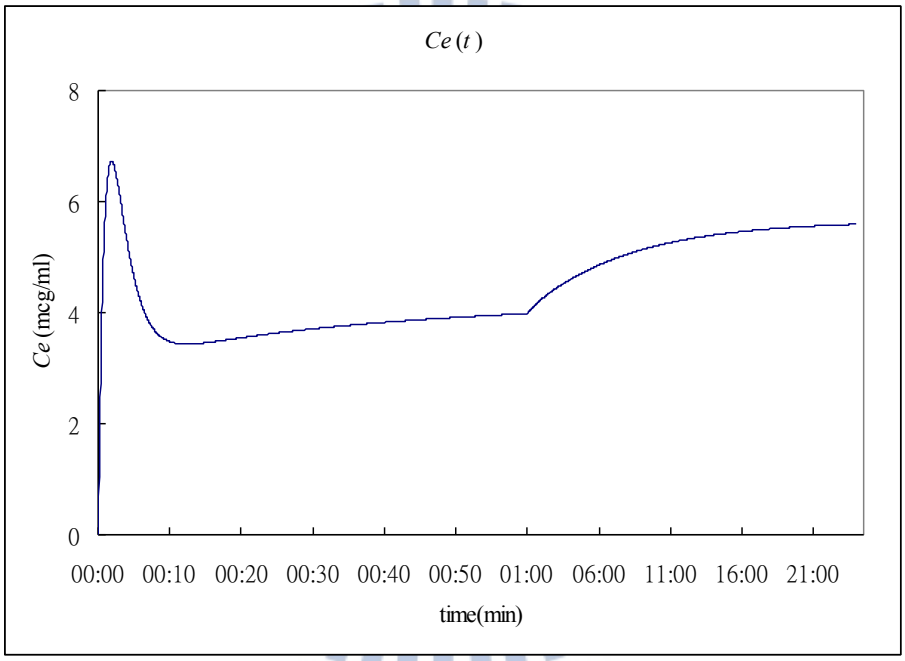

Figure 5. The propofol *Ce* trend with 4 extrema. It is produced by a loading bolus injection (100 mg) and a constant rate infusion (10 mg/min) start from the injection time.

The simlations below were coded in NetBean IDE 6.5 and tested on a java ME platform for a SonyErricson cell phone, type w660i. The drug selected for simulation was propofol. It was selected for its quick onset and offset so that the guider needed to calculate its *Ce* trend faster than most of the other drugs. A very widely used PopPK model of Schnider was selected [17]. The simulated object was a 52-years-old, 68.5 kg, 167 cm height male based on the average values or the major gender of Schnider's objects. The t_{peak} time, an important PD property, was choosed as 1.6 minutes according to his another study [39].

The injection and infusion history of propofol in simulation 1 was a combination of a

loading bolus injection of 100 mg and a constant rate infusion of 10mg/min started at that injection time. This simple administration history produced *Ce* trend with 4 extrema. Theoretically, trying to plot *Ce* trend with more extrema takes longer time using the RRI algorithm [appendix 12-13].

The time domain on trail varies from 10 to 10^9 seconds. So sampling point numbers (n_{sp}-s) were 100, 10^3, ... 10^9 separately. The time needed to plot *Ce* trend by way of different algorithm within different size of time-domains was tested for 10 times. The time was compared between the three algorithms with Student's t-test for different size of time-domains.

3.2. Simulation 2. How long it takes to search for an optimal injection dose.

This simulation compared the efficiency of linear search and bisection method search for optimal injection dose. The platform, the simulated object, the drug, the PopPK model and the t_{peak} were identical to simulation 1. The *Cet* was 4mcg/ml. The *Cet* percentage range was 10%.

After a serial of drug administration, t_0 is the time to find an optimal injection dose. Let $TMax(d)$ be the maximum value of *Ce* trend following the injected dose d at time t_0 and UB be the upper bound of *Cet* range. Let *Pu* be the peak value after the injection of one unit dose to an object without any drug in its body and *Qd* be the step quantity of injection dose. Optimal injection dose is defined as the maximal d that satisfies $TMax(d) \leq UB$. Because of the additive property of *Ce* functions, $\left\lfloor \frac{UB}{Pu \cdot Qd} \right\rfloor \cdot Qd$ is an upper bound of d.

The simulated administration history was a single bolus injection that elevates *Ce* to a peak within the *Cet* range, and t_0 was the time of *Ce* peak. To search this optimal injection dose is the worse case for both linear search and bisection method. To search for the initial loading dose is not selected as a simulation history because it is the best case of linear search by the definition of its upper bound of injected dose.

In linear search, d was verified iteratively from its upper bound, $\left\lfloor \frac{UB}{Pu \cdot Qd} \right\rfloor \cdot Qd$, and substracted a *Qd* from d for each iteration until $TMax(d) \leqq UB$ or $d \leqq 0$. In bisection method the initial upper bound of d was the same as linear search and the initial lower bound was 0 [appendix 14]. Various values of *Qd* (0.1, 0.2, 0.3, 0.5, 1, 2, 3, 5 ml of 10mg/ml propofol)

were tested for both algorithms. Each algorithm-*Qd* item was tested for 10 times and the time to find out optimal injection dose was recorded. Because this injection dose was 0, both methods encountered their worst case. The most efficient method to calculate *Ce* trend in simulation 1 was used to get the values of *TMax*(*d*). The times needed to find out optimal injection dose with both algorithms were compared with Student's t-test.

3.3. Simulation 3. How long it takes to search for an optimal infusion rate.

This simulation compared the efficiency of linear search and bisection method search for optimal infusion rate. The platform, the simulated object, the drug, the PopPK model and the t_{peak} were identical to simulation 1. The *Cet* was 4mcg/ml. The *Cet* percentage range was 10%.

After a serial of drug administration, t_0 is a time to find an optimal infusion rate. Let *TMin*(*r*) be the minimal value of *Ce* trend produced by setting the infusion rate to *r* at time t_0 and *LB* be the lower bound of *Cet* range. Optimal infusion rate is defined as the minimal *r* value that satisfies $TMin(r) \geqq LB$. The upper bound of *r* is specified by the pump used to infuse the drug.

As we learned from simulation 2, the initial injection dose 74 mg produced a *TMax* closer to *UB* than any other initial injection dose. So we simulated the administration history as a single bolus injection of 74 mg propofol that elevate *Ce* to a peak value within the *Cet* range, and t_0 was the time of *Ce* peak. Let *Qr* be the step quantity of infusion rate. In linear search, *r* was verified iterately from 0 to its upper bound stepped *Qr* until $TMin(r) \geqq LB$. The upper bound of *r* was defined as 999.9 ml/hr as most of commercially available syringe pumps or infusion pumps. In bisection method search [appendix 15] the initial upper bound of *r* was the same as linear search and the initial lower bound was 0. Various values of *Qr* (0.1, 0.2, 0.5, 1, 2, 5 ml/hour of 10 mg/ml propofol) were tested. Each algorithm-*Qr* item was tested for 10 times and the time to find out optimal infusion rate was recorded. The most efficient method to calculate *Ce* trend in simulation 1 was used to get the values of *TMin*(*r*). The times needed to find out the optimal infusion rate with both algorithms were compared with Student's t-test.

Whether the workload to maintain *Ce* in *Cet* range is reasonable for manual control is to be determined in the next two simulations. The TCMII guider provides two strategies. Firstly, when there is no available pump, a user can inject drug again and again. Secondly, when a pump is available, a user can inject a loading dose and repeatedly adjust the infusion rate.

3.4. Simulation 4. The frequency of injecting optimal dose to maintain *Ce*

The platform, the simulated object, the drug, the PopPK model and t_{peak} were identical to simulation 1. The *Cet* was setted to 4mcg/ml. Whenever *TMax* was lower than *LB*, the guider showed an optimal injection dose and reminded the user through audio alarms. The user was simulated to inject that dose of propofol into the object instantly. By repeating this step, *Ce* was maintained in the *Cet* range for an hour. Various commonly used *Qd*-s (0.1, 0.2, 0.3, 0.5, 1, 2, 3, 5ml) and various *Cet* ranges (1, 2, 3, 5, 10, 15, 20, 30, 50%) were tested. The numbers of injections in the first hour were recorded. A reasonable number of injections in the first hour was defined as 30 or once per two minutes on average.

3.5. Simulation 5. The frequency of setting optimal infusion rate to maintain *Ce*

The platform, the simulated object, the drug, the PopPK model and t_{peak} was identical to simulation 1. The *Cet* was setted to 4mcg/ml. The initial injection dose was an optimal dose which produced a peak *Ce* value at time t_{peak} and drive *Ce* close to *UB*. The optimal infusion rate value was calculated on the time t_{peak} and infusion was simulated to run at the optimal rate from the time t_{peak}. The guider recalculated optimal infusion rate and and reminded the user through audio alarms whenever *TMin* was going to be higher than *UB*. The user reseted the infusion rate to the new optimal rate instantly. By repeating this, *Ce* was maintained in *Cet* range steadily. Various commonly used *Qr*-s, step values of infusion rates, (0.1, 0.2, 0.5, 1, 2, 5ml/hr) were tested. Various *Cet* percentage ranges (1, 2, 3, 5, 10, 15, 20, 30, 50%), were tested. The numbers of rate-changing were recorded. A reasonable interval of rate-changing is defined as 10 minutes.

Chapter 4: Results

4.1. Simulation 1. How long it takes to plot *Ce* trend.

The average times needed to plot *Ce* trend with ALS, NLS and RRI algorithms were listed in table 3 and plotted in figure 6. When n_{sp} is less than 100, or time domain size is less than 100 seconds, the three algorithms are all feasible for manual guide. When n_{sp} is less than 10^3, or time domain size is about 15 minutes, NLS and RRI is still feasible. But when n_{sp} is more than 10^4, or time domain size is about 3 hours, neither ALS nor NLS is feasible. RRI can plot *Ce* trend in 30 ms for n_{sp} to be 100 to 10^9, or for time domain size to be up to 32 years. The t-tests between pairs demonstrate significant difference. The p values were all less than 0.05 except the difference between NLS-RRI when n_{sp} was 100.

According to the result of simulation 1, the following simulations use RRI to calculate *Ce* trend.

4.2. Simulation 2. How long it takes to search for an optimal injection dose.

The average time it takes to search for an optimal dose with linear search and bisection method algorithms was listed in table 4 and plotted in figure 7. Under all of the situations, linear search and bisection method were feasible to guide manual injections except when *Qd* was setted to be 0.1. Statistcally, bisection method is more efficient than linear search ($p<0.05$). The following simulations (simulation 3, 4 & 5) used bisection method to search for optimal injection doses.

4.3. Simulation 3. How long it takes to search for an optimal infusion rate.

The average times needed to search for an optimal infusion rate with linear search method and bisection method algorithms were listed in table 5 and plotted in figure 8. Linear search was feasible to search for optimal infusion rate only when *Qr* was equal to 2 or 5. Using bisection method we find out optimal infusion rate within 1 second that was statistically better than using linear search ($p<0.05$). In simulation 5 we used bisection method to find out optimal infusion rate.

4.4. Simulation 4. The frequency of injecting optimal dose to maintain *Ce*

How many times an optimal dose is injected to keep *Ce* in *Cet* ranges in the first hour were listed in table 5 and plotted in figure 9. To find an optimal injection dose for a narrower *Cet* range, a smaller *Qd* and more frequent injections were needed. When *Cet* range is not less than 10%, the frequency of injection to maintain *Ce* was reasonable for manual workload. The size of *Qd* was not related to the frequency of injections but larger *Qd* needed larger *Cet* percentage ranges to get a proper injection dose.

4.5. Simulation 5. The frequency of setting optimal infusion rate to maintain *Ce*

First, when the *Cet* range was smaller, a smaller *Qr* and more frequent of adjustment of infusion rate was needed. Second, as time goes by, the interval beween adjustment of infusion rate was getting longer. The numbers needed to change the infusion rate to keep *Ce* in *Cet* ranges were listed in table 7 and plotted in figure 10. All of the average frequencies to change rate to change were less than once per 10 min. When the *Cet* range was equal to or greater than 5%, the average frequencies to change rate were less than once per 30 min. In fact the number of setting infusion pump running at optimal rate to keep *Ce* in *Cet* range infinitely is less than 4 when *Cet* percentage range is 10%. The numbers of setting infusion pump running at optimal rate to keep *Ce* in various *Cet* percentage range infinitely were listed in table 8 and plotted in figure 11.

Table 2. How long it takes to search for all of the extrema of *Ce* trend by analytical linear search, numerical linear search and real root isolation algorithms.

nsp	*tALS(ms)*	*tNLS(ms)*	*tRRI(ms)*	*p(ALS-NLS)*	*p(ALS-RRI)*	*p(NLS-RRI)*
100	28	2.8	2.9	<0.001	<0.001	0.67
103	330	26	24	<0.001	<0.001	<0.001
104	3800	280	30	<0.001	<0.001	<0.001
105	36000	2700	29	<0.001	<0.001	<0.001
106	#	28000	29	#	#	<0.001
107	#	#	29	#	#	#
108	#	#	29	#	#	#
109	#	#	29	#	#	#

n_{sp}: The number of sampling points. The sampling interval is one second and the time domain width is n_{sp} seconds.
tALS: The average time needed to get Ce value using analytical method and to explore the Ce extrema using linear search method.
tNLS: The average time needed to get Ce value using numerical method and to explore the Ce extrema using linear search method.
tRRI: The average time needed to get Ce value using analytical method and to explore the Ce extrema using recursive root isolation method with pseudo-derivative sequence, and bisection method.
p(ALS-NLS): The independent two-tailed test p-value of equality of the means of tALS and tNLS.
p(ALS-RRI): The independent two-tailed test p-value of equality of the means of tALS and tRRI.
p(NLS-RRI): The independent two-tailed test p-value of equality of the means of tNLS and tRRI..
#: not tested, no data

Table 3. How long it takes to search for an optimal injection dose by linear search and bisection method

***Qd*(ml)**	***t*LS(ms)**	***t*BM(ms)**	**p**
0.1	1660	279	<0.001
0.2	878	207	<0.001
0.5	394	167	<0.001
1	258	114	<0.001
2	173	76	<0.001
5	81	44	<0.001

Qd: The step quality of injection dose.
*t*LS: the time to do linear search for optimal injection dose.
*t*BM:the time to use bisection method for optimal injection dose.

Table 4. How long it takes to search for an optimal infusion rate by linear search and bisection method

Qr(ml/hr)	*t*LS(ms)	*t*BM(ms)	p
0.1	15600	568	<0.001
0.2	6370	451	<0.001
0.5	3210	394	<0.001
1	1670	337	<0.001
2	700	271	<0.001
5	398	227	<0.001

Qr: The step quality of infusion rate
*t*LS: the time to do linear search for optimal infusion rate
*t*BM:the time to use bisection method to search for optimal infusion rate

Table 5. How many times an optimal dose is injected to keep *Ce* in *Cet* ranges in the first hour

range(%) / *Qd*(ml/hr)	1%	2%	3%	5%	10%	15%	20%	30%	50%
0.1	86	59	48	37	25	20	17	14	9
0.2	93	63	50	38	26	21	18	14	9
0.3	#	#	52	41	27	21	18	14	9
0.5	#	#	#	42	27	21	18	14	10
1	#	#	#	59	32	23	18	14	10
2	#	#	#	#	#	31	22	16	10
3	#	#	#	#	#	23	22	21	10
5	#	#	#	#	#	#	#	15	11

range(%): *Cet* percentage range
Qd: The step quality of injection dose
#: these is no proper injection dose to keep *Ce* in the *Cet* percentage range

Table 6. The average of optimal maintenance doses in simulation 4 while *Qd* = 0.1 ml

Cet range	average optimal maintenance dose
1%	0.7
2%	1.1
3%	1.4
5%	1.8
10%	2.7
15%	3.4
20%	4.0
30%	5.2
50%	7.5

Qd: The step quality of injection dose.

Table 7. How many times the infusion rate is setted optimally to keep *Ce* in *Cet* range in the first two hours

range(%) / Q_r (ml/hr)	1%	2%	3%	5%	10%	15%	20%	30%	50%
0.1	8	5	4	3	2	2	2	1	1
0.2	8	5	4	3	2	2	2	1	1
0.5	8	5	4	3	2	2	1	1	1
1	9	6	4	3	2	2	1	1	1
2	10	6	5	3	2	2	1	1	1
5	#	#	6	4	2	2	1	1	1

range(%): Cet percentage range
Qr: The step quality of infusion rate
#: these is no proper infusion rate to keep *Ce* in the *Cet* percentage range

Table 8. How many times the infusion rate is setted optimally to keep *Ce* in *Cet* range infinitely..

range(%) / Q_r (ml/hr)	1%	2%	3%	5%	10%	15%	20%	30%	50%
0.1	15	9	7	5	3	2	2	1	1
0.2	15	9	7	5	3	2	2	1	1
0.5	16	10	7	5	3	2	2	1	1
1	24	10	7	5	3	2	2	1	1
2	#	12	8	5	3	2	2	1	1
5	#	#	#	#	4	3	2	2	1

range(%): *Cet* percentage range
Qr: The step quality of infusion rate
#: these is no proper infusion rate to keep *Ce* in the *Cet* percentage range

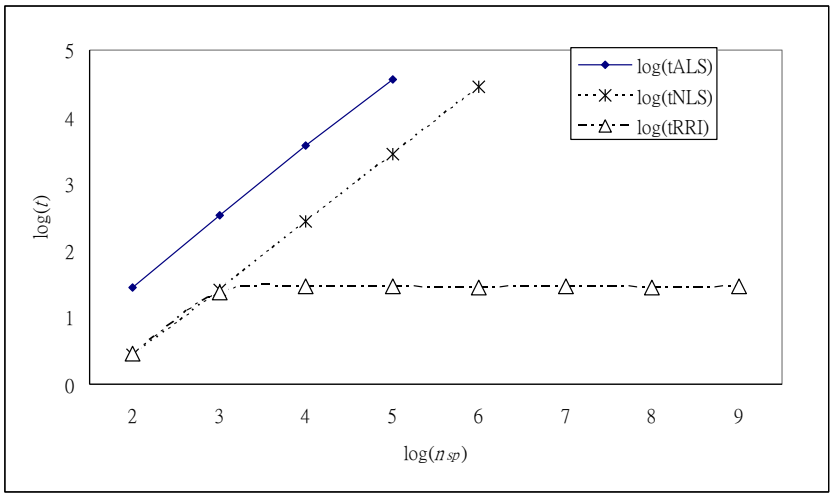

Figure 6. How long it takes to search for all of the extrema of *Ce* trend by analytical linear search, numerical linear search and real root isolation algorithms in various size of time domain

n_{sp}: The number of sampling points. The sampling frequence is 1 Hz.
tALS: How long it takes to get *Ce* value using analytical method and to find *Ce* extrema by linear search.
tNLS: How long it takes to get *Ce* value using numerical method and to find *Ce* extrema by linear search.
tRRI: How long it takes to get *Ce* value using analytical method and to find *Ce* extrema by real root isolation method, and bisection method.

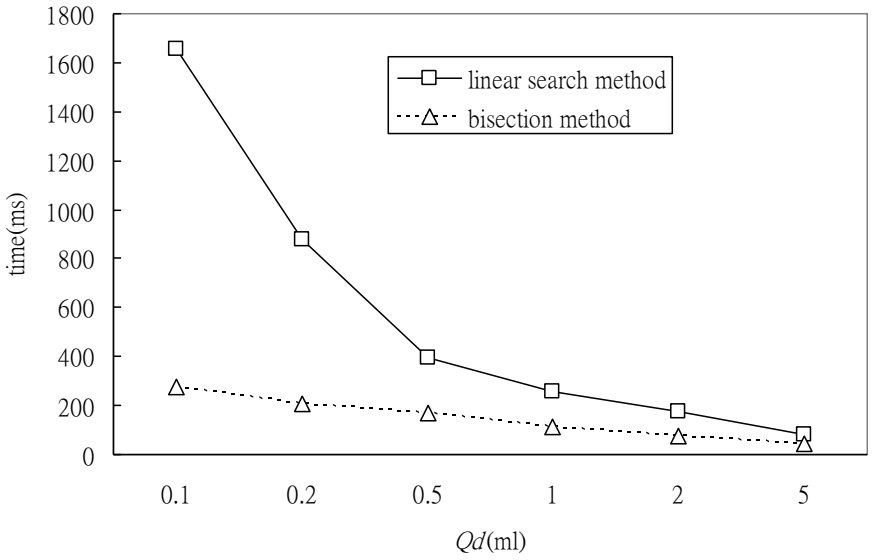

Figure 7. How long it takes to search for an optimal injection dose by linear search and bisection method

Qd: The step quality of injection dose

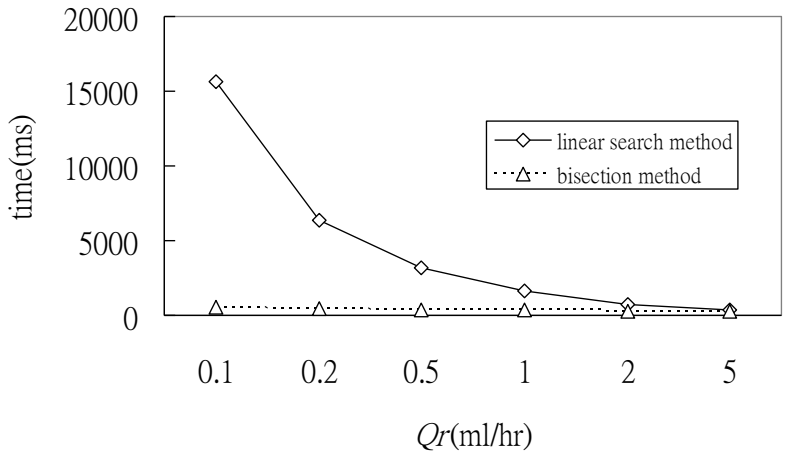

Figure 8. How long it takes to search for an optimal infusion rate by linear search and bisection method.
Qr: The step quality of infusion rate

(a)

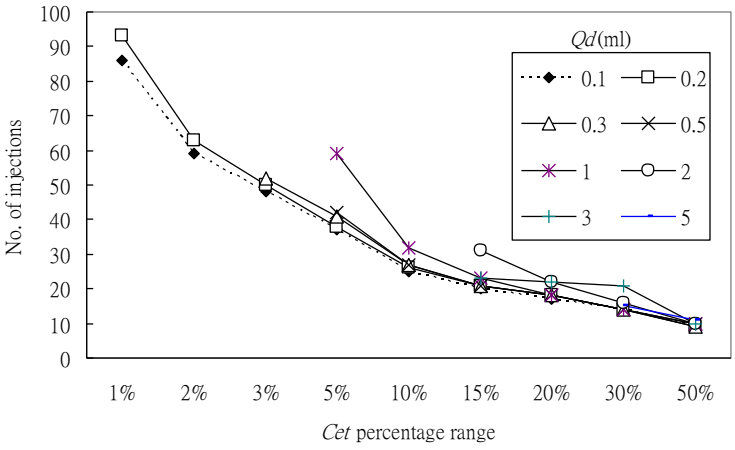

(b)

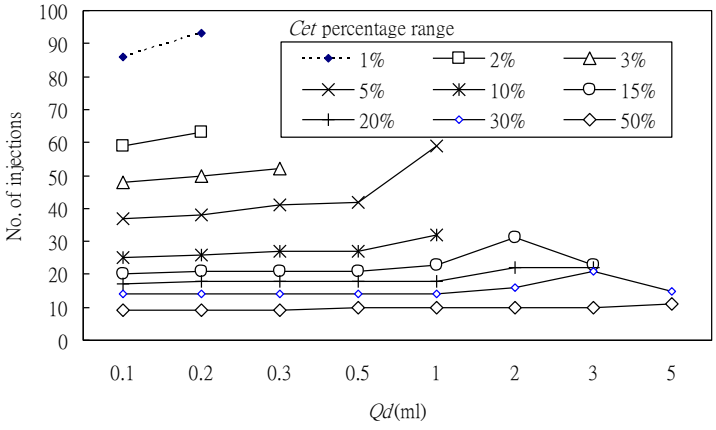

Figure 9. How many times an optimal dose is injected to keep *Ce* in *Cet* range for an hour.
Qd: The step quality of injection dose.

(a)

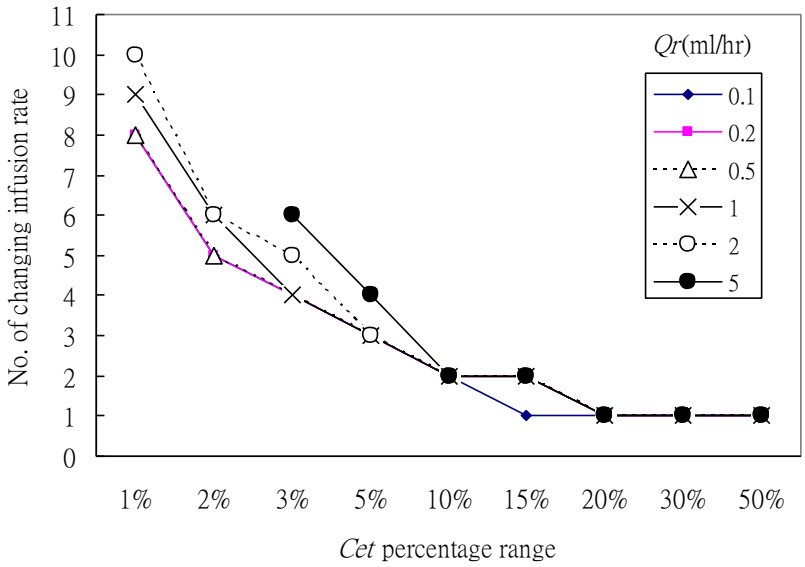

(b)

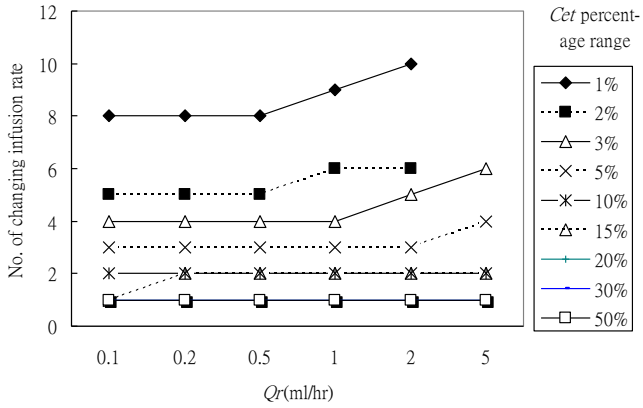

Figure 10. How many times the infusion rate is setted optimally to keep *Ce* in *Cet* range in the first two hours.
Qr: The step quality of infusion rate

(a)

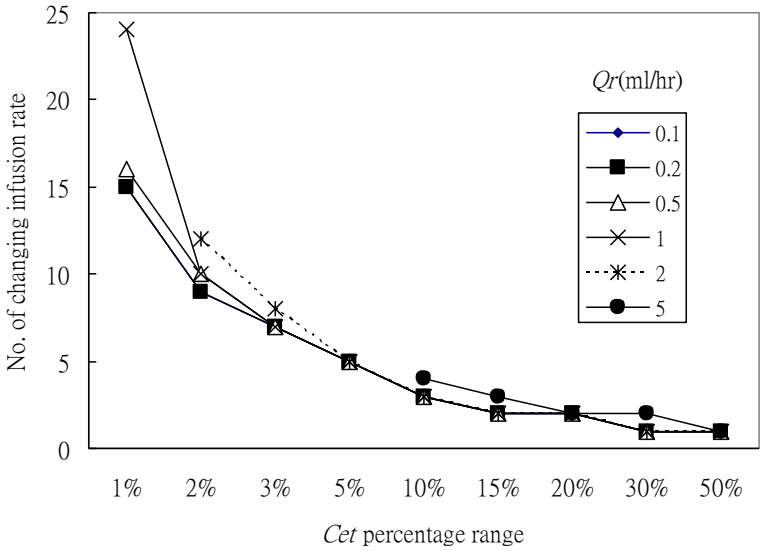

(b)

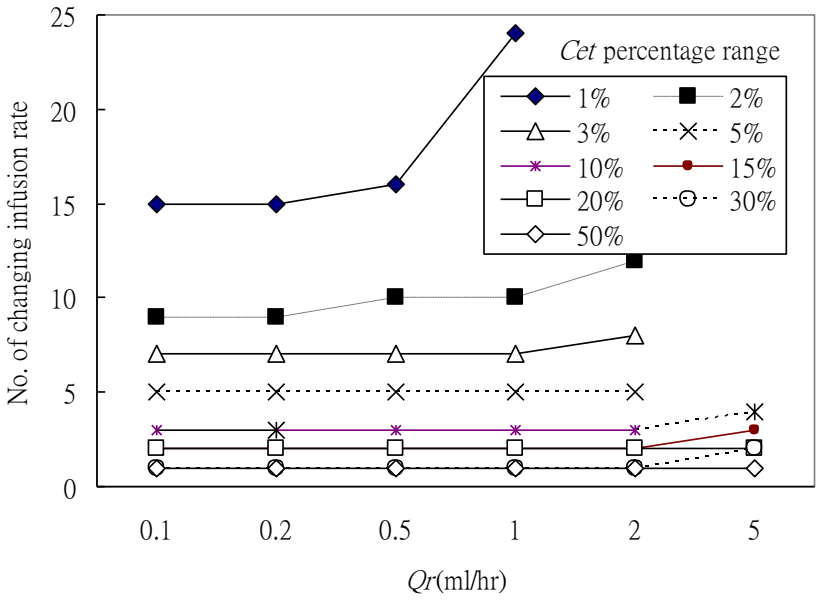

Figure 11. How many times the infusion rate is setted optimally to keep *Ce* in *Cet* range infinitely
Qr: The step quality of infusion rate

Chapter 5: Discussion

5.1. System evaluation and findings

These simulations are designed to evaluate and to select the algorithms that are essential to build a TCMII guider. *Ce* trend can help a user to foretell the effect of drug administration and enable the guider to compare between the administrations of drug about how long the *Ce* is kept in its target range. The efficiency of algorithms to plot *Ce* trend is evaluated in simulation 1 and the real root isolation method is the best choice especially when the time range to forecast is very large. The efficiency of algorithms to search for an optimal injection dose is evaluated in simulation 2 and the bisection method is found better although linear search method is also efficient enough to calculate optimal doses timely. The efficiency of algorithms to search for an optimal infusion rate is evaluated in simulation 3 and only the bisection method is found efficient enough to calculate optimal rates timely although not good enough to handle several drugs simultaneously on the tested platform. The feasibility of the strategy of administering optimal injection doses repeatedly is tested in simulation 4. This strategy was found plausible because the frequency of injection was not higher than manual injection without guide. Moreover, using a guider can maintain *Ce* steadily and change *Cet* range according to clinical situation. The feasibility of the strategy of repeatedly setting infusion rate optimally is tested in simulation 5 and found plausible because the frequency of setting is far less than manual infusion without guide and *Ce* is kept steady with a guider.

Analytical linear search (ALS) and numerical linear search (NLS) are inefficient when the time domain is wider larger than 10^4 seconds (around 2.8 hours). On the other hand, real root isolation (RRI) method is efficent for a time domain size up to 100 to 10^9 seconds (around 32 years).

How large the time domain of *Ce* trend is large enough for manual control? Based on the data of simulation 5, the interval between two infusion rate changings can be as long as 9.5 hours (*Cet* percentage range = 5%, *Qr* = 0.1ml/hr). ALS and NLS can not figure *Ce* trend in 0.2 second when the size of time domain is 9.5 hours. RRI can figure *Ce* trend in 30 ms so it is a reasonable choice of the method to find out *TMin* and *TMax* in the following simulations.

NLS works well when the size of time domain is less than 10^3 seconds (16 minutes). This is why NLS can be applied on TCI systems, because the t_{peak} of most of the drugs in TCI is within several minutes and the time domain size of *Ce* trend of TCI is t_{peak} plus 10 seconds as mentioned in section 2.5. The issues of accumulation of rounding error and occilation are not

significant in this simulation.

To be a guider of manual administration, a TCMII needs to predict *Ce* trend on a much larger time domain than that of a TCI system. It was difficult in the past is now possible with RRI method.

Either to use TCMII guider as an assistant tool or as a guider, showing extrema to users is as good as showing the whole *Ce* trend. The key point is that *Ce* extrema can be calculated much faster than the whole sampling points of *Ce* trend.

The RRI algorithm finds the roots of three or four degree multi-exponential function efficiently. It is infered that this algorithm can solve even higher degree multi-exponential function problems. Using this algorithm we might be able to calculate *Ce* trend of PK models with more compartments such as inhalational drug PK models.

In simulation 2, to find the *TMax* of all candidate injection doses is the most time-consuming process to search for an optimal dose. A smaller *Qd* needs to calculate *TMax* more times either for linear search or bisection method. Linear search is feasible except when *Qd* is 0.1ml, however such a small *Qd* is seldom used on clinical application of propofol. Bisection method is more efficient than linear search and is the choice of the method to find an optimal injection dose in simulation 4.

In simulation 3, to find *TMin* is the the most time-consuming process in searching optimal infusion rate. Since most of the infusion pumps can be set to 0.1ml/hr, it is unreasonable to limit *Qr* greater than 0.1ml/hr. However, using smaller *Qr* means to test more candidate rates and to calculate *TMin* more times. Linear search is feasible only when *Qr* is greater than 1ml/hr. Bisection method is feasible for all *Qr*-s from 0.1 to 5 ml/hr. However when *Qr* is 0.1ml/hr, the speed to search for an optimal infusion rate (=0.6 second) is not quick enough to handle several different drugs in the same time. It should be improved in the future study.

In simulation 4, table 5 and figure 9 demonstrated that to select *Cet* percentage range below 5% calls for frequent intermittent injections which is inconvinient for long term administration. But it is good at the epilog of a procedure when we need to taper the *Ce* adapting the less stimulating treatments such as skin suture or gauze dressing. It helps to shorten the time between weaning off injections and awakening.

Cet range must be higher than effective concentration and lower than toxic level. It is supposed to be adjusted according to clinical situations. Setting *Qd*, limited to the precision of manual injection, to 0.5 or 1 ml are feasible options. Setting *Cet* percentage range, according

to the data in table 6 and propofol label [40], to 10-20% is reasonable because 2.5-5ml supplemental maintaining injection dose of propofol is safely used in clinical practice. The *Cet* percentage range values need furthor clinical investigation.

In simulation 4 and 5, we arbitrarily define a feasible frequence for intravenous anesthesia administration depending on clinical experience. The average frequencies of adjustment of infusion rate in the first two hours were taken to stand for workloads in anesthesia and the frequency of adjustment to keep Ce stand for workloads in long-term sedation. In this research we test propofol, one of the most quickly onset/offset drug, and obtained feasible stratagies of manual administration. We believe that this guider and these stratagies are feasible for most of the intravenous drugs. Especially when simulation 5 revealed that to keep *Ce* in a reasonable *Cet* range (5% to 20%) with an infusion pump need to change the infusion rate only few times. It means that a TCMII guiding infusion can do long-term *Ce* control conveniently where TCI pump is not available.

5.2. Limitations

This research studies only the simulations of the PopPK model of propofol presented by Schnider. Propofol is one of the most popular drugs to be controlled with PK PD model and also a drug with rapid *Ce* change that needs a rapid search for optimal injection dose and infusion rate. If TCMII guider handles propofol well, it handles other drugs well, too. But the PK PD models of other drugs or the other PK PD models of propofol is not tested in this preliminary study and need further efforts.

The difference between the time to input dose/rate data into TCMII guider and the time to push the dose or set the infusion rate is ignored. How these timing errors influence the accuracy of *Ce* values is left to future studies.

5.3. Contributions

Because manual-controlled drug administration is not totally replaced by computer -controlled equipment, it is helpful to develop a manual-controlled guider. Such a guider was unfeasible in the past because the calculation of a long term *Ce* trend needs a high efficient algorithm. We introduced a real root isolation method to solve the problem of finding the roots and extrema of a multiple exponential function and to solve the problem of finding *Ce* trend of a serial of manual drug administrations. This method can further combined with bisection method to resolve the problem of searching for optimal injection dose and optimal infusion rate timely. These algorithms are efficient enough to work on handheld devices and

enable the utilization of PopPK models on demand and give quantitative suggestion for specific cases. Other than these suggestions, this guider accepts any user's manual administration plan and presents *Ce* trend to foretell the drug effect.

This method is more elastic and complies with clinical demand better than traditional 'ten-eight-six' regimen [29]. TCMII tames the rapid fluctuations in *Ce* following intermittent injections and sharpens the response of manual infusion to clinical requirement.

Chapter 6: Conclusion

TCI was the only technique for *Ce* controlling until TCMII was developed. This research provides an alternative way to control *Ce* based on the same PopPK model. The simulations demonstrated that a proper *Cet* range is or can be infered from current clinically used step quantity of injection doses. The workload induced from a proper *Cet* range is acceptable for human. TCMII guider has the potential to help a user to do manual injection and infusion elaborately.

References

1. Campbell L, “Total intravenous anaesthesia”, CPD Anaesthesia **3(3)**:109-119, 2001.
2. Shafer SL, Gregg KM, “Algorithms to rapidly achieve and maintain stable drug concentrations at the site of drug effect with a computer-controlled infusion pump”, J Pharmacokinetics and Biopharmacokinetics **20(2)**:147, 1992.
3. Sahinovic MM, Absalom AR, Struys MM, “Administration and monitoring of intravenous anesthetics”, Current Opinion in Anesthesiology, **23(6)**:734-40, 2010.
4. Shafer SL, “Towards Target Controlled Drug Delivery”, Available at http://www.slidefinder.net/t/towards_target_controlled_drug_delivery/30531182.
5. Egan TD, Shafer SL, “Target-controlled infusions for intravenous anesthetics - Surfing USA not!”, Anesthesiology **99**:1039–41, 2003.
6. Pandit JJ, “Intravenous anaesthetic agents”, Anaesthesia and Intensive Care Medicine **9(4)**:154-159, 2007.
7. Shafer SL, Siegel LC, Cooke JE, Scott JC, “Testing computer-controlled infusion pumps by simulation”, Anesthesiology **68(2)**:261-6, 1988.
8. Xu M, Chen LY, Zeng ZB and Li ZB, “Real root isolation of multi-exponential polynomials with application”, Proceedings of the Workshop on Algorithms and Computation - Lecture Notes in Computer Science(WALCOM LNCS 2010) **5942**:263–268, 2010.
9. Burton ME,Shaw LM,Schentag JJ,Evans WE, “Applied pharacokinetics and pharacodynamics”, Principles of Therapeutic Drug Monitoring, fourth ed. printed by Lippincott Williams & Wilkins, pp. 41–45, 2006.
10. Naidoo D, “Target controlled infusions”, Available at http://anaesthetics.ukzn.ac.za/Libraries/Documents2011/D_Naidoo_Target_Controlled_Infusion.sflb.ashx.
11. Brain-Gut Research Group, “Pharmacokinetics study”, Available at http://www.braingut.com/pharmacokinetics. asp.
12. Wikipedia, “Multi-compartment model”, Available at http://en.wikipedia.org/wiki/Multi-compartment_model.
13. U.S. Department of Health and Human Services FDA CDER CBER: Guidance for industry population pharmacokinetics, 1999.
14. Bonate PL, “Recommended reading in population pharmacokinetic pharmacodynamics”, The AAPS Journal **7(2)** Article 37:E363-73, 2005.
15. Heeremans EH, Proost JH, Eleveld DJ, Absalom AR, Struys MM, “Population pharmacokinetics and pharmacodynamics in anesthesia, intensive care and pain medicine”, Current Opinion in Anesthesiology **23(4)**:479-84, 2010.
16. Krüger-Thiemer E, “Continuous intravenous infusion and multicompartment accumulation”, European Journal of Pharmacology **4**:317–24, 1968.

17. Schnider TW, Minto CF, Gambus PL, Andresen C, Goodale DB, Shafer SL, Youngs E, "The influence of method of administration and covariates on the pharmacokinetics of propofol in adult volunteers", Anesthesiology **88(5)**:1170-82, 1998.

18. Hull CJ, Van Beem HB, McLeod K, Sibbald A, Watson MJ, "A pharmacodynamic model for pancuronium", British Journal of Anaesthesia **50**:1113-23, 1978.

19. Sheiner LB, Stanski DR, Vozeh S, Miller RD, Ham J, "Simultaneous modeling of pharmacokinetics and pharmacodynamics: application to d-tubocurarine", Clinical Pharmacology & Therapeutics **25**:358-71, 1979.

20. Gepts E, "Pharmacokinetic concepts for TCI anaesthesia", Anaesthesia **53** Suppl 1:4-12, 1998.

21. Guarracino F, Lapolla F, Cariello C, Danella A, Doroni L, Baldassarri R, Boldrini A, Volpe ML, "Target controlled infusion: TCI", Minerva Anestesiologica **71(6)**:335-7, 2005.

22. Ausems ME, Vuyk J, Hug CC Jr, Stanski DR, "Comparison of a computer-assisted infusion versus intermittent bolus administration of alfentanil as a supplement to nitrous oxide for lower abdominal surgery", Anesthesiology **68(6)**:851-61, 1988.

23. Ting CH, Arnott RH, Linkens DA, Angel A, "Migrating from target-controlled infusion to closed-loop control in general anaesthesia", Computer Methods and Programs in Biomedicine **75**:127-139, 2004.

24. Asbury AJ, "Feedback control in anaesthesia", International Journal of Clinical Monitoring and Computing **14 (1)**:1-10, 1997.

25. Glass PSA, Shafer SL, Jacobs JR, Reves JG, "Intravenous drug delivery systems", Miller's Anaesthesia, fourth ed. printed by Churchill Livingstone, 1994.

26. Rinehart J, Liu N, Alexander B, Cannesson M, "Closed-loop systems in anesthesia: is there a potential for closed-loop fluid management and hemodynamic optimization?", Anesthesia & Analgesia **114(1)**:130-43, 2012.

27. Bailey JM, "An approximate model-independent method to maintain constant plasma levels of intravenous drugs", Journal of Pharmacokinetics and Biopharmaceutics **19(6)**:635-45, 1991.

28. Struys M, Versichelen L, Thas O, Herregods L, Rolly G, "Comparison of computer-controlled administration of propofol with two manually controlled infusion techniques", Anaesthesia **52(1)**:41-50, 1997.

29. Roberts FL, Dixon J, Lewis GT, Tackley RM, Prys-Roberts C, "Induction and maintenance of propofol anaesthesia - A manual infusion scheme", Anaesthesia **43**(Supplement):14–7, 1988.

30. Gale T, Leslie K, Kluger M, "Propofol anaesthesia via target controlled infusion or manually controlled infusion: effects on the bispectral index as a measure of anaesthetic depth", Anaesthesia and Intensive Care Journal **29(6)**:579-84, 2001.

31. Raemer DB, Buschman A, Varvel JR, Philip BK, Johnson MD, Stein DA, Shafer SL, "The prospective use of population pharmacokinetics in a computer-driven infusion system for alfentanil", Anesthesiology **73(1)**:66-72, 1990.

32. Maitre PO, Ausems ME, Vozeh S, Stanski DR, Evaluating the accuracy of using population pharmacokinetic data to predict plasma concentrations of alfentanil, *Anesthesiology* **68**:59-67, 1988.

33. Jacobs JR, Analytical solution to the three-compartment pharmacokinetic model, *IEEE Transactions on Biomedical Engineering* **35**:763-5, 1988.

34. Bailey JM, Shafer SL, A simple analytical solution to the three-compartment pharmacokinetic model suitable for computer-controlled infusion pumps. *IEEE Transactions on Biomedical Engineering* **38(6)**:522-5, 1991.

35. Hemmerling TM, Charabati S, Zaouter C, Minardi C, Mathieu PA, A randomized controlled trial demonstrates that a novel closed-loop propofol system performs better hypnosis control than manual administration, *Canadian Journal of Anesthesia* **57**:725–735, 2010.

36. Moore BL, Quasny TM, Doufas AG, Reinforcement learning versus proportional-integral- derivative control of hypnosis in a simulated intraoperative patient, *Anesthesia & Analgesia* **112(2)**:350-9, 2011

37. Maurer WG, Philip BK, Propofol Infusion Platforms: Opportunities and Challenges, *Digestion* 82:127–129, 2010.

38. Moore BL, Pyeatt LD, Doufas AG, Fuzzy control for closed-loop, patient-specific hypnosis in intraoperative patients: a simulation study, *Conference Proceedings - IEEE Engineering in Medicine and Biology Society* pp. 3083-6, 2009.

39. Schnider TW, Minto CF, Shafer SL, Gambus PL, Andresen C, Goodale DB, Youngs EJ, The influence of age on propofol pharmacodynamics, *Anesthesiology* **90(6)**:1502-16, 1999.

40. Bedford Laboratories, Label of propofol. Available at http://dailymed.nlm.nih.gov/dailymed/drugInfo.cfm?id=6337.

Appendices

Appendix 1. Three-compartment mammillary model

It is assumed that the given drug mixed in central compartment instantly and the accumulated mass in central compartment is A_1. Then the drug is either elimiated through metabolic organs at the rate of $k_{10}\cdot A_1$ (let CL_1 be the metabolic clearance, $k_{10} = CL_1 / V_1$) or is transported to other organs (compartment i) at the rate of $k_{1i}\cdot A_1$ (let CL_i be the distributional clearance of compartment i, and $k_{1i} = CL_i / V_1$). The drug in compartments, other than compartment 1, transfers back to compartment 1 at the rate of $k_{i1}\cdot A_i$ ($k_{i1} = CL_i / V_i$). These descriptions are summarized into the differential eq. set (10)

$$\begin{cases} \dfrac{dA_1}{dt} = r + k_{21}A_2 + k_{31}A_3 - (k_{12} + k_{13} + k_{10})A_1 \\ \dfrac{dA_2}{dt} = k_{12}A_1 - k_{21}A_2 \\ \dfrac{dA_3}{dt} = k_{13}A_1 - k_{31}A_3 \end{cases} \tag{10}$$

if r denotes the infusion rate of the drug.

Let $\hat{f}(s)$ denote the Laplace transform of a function $f(t)$. The application of the Laplace transform to both sides of differential eq. set (10) yields a system of equations, eq. set (11), that are all linear in the $\hat{A}_i(s)$.

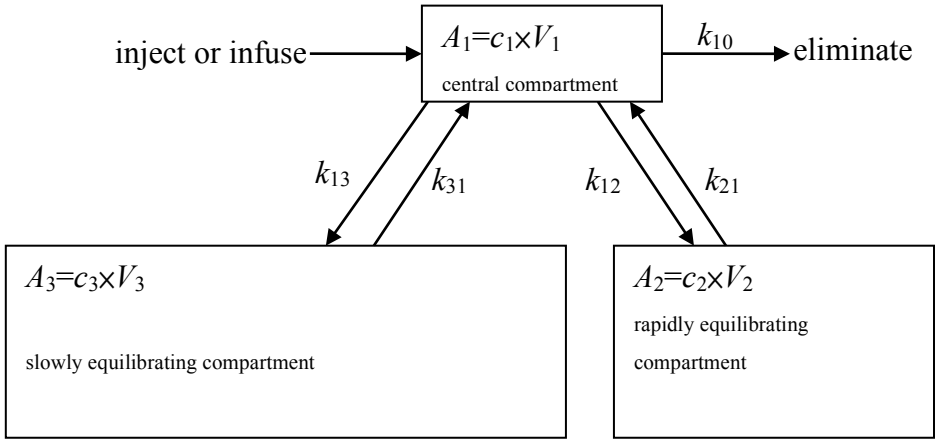

Figure 12. Three-compartment PK model

$$\begin{cases} s\hat{A}_1 - A_1(0) = \dfrac{r}{s} + k_{21}\hat{A}_2 + k_{31}\hat{A}_3 - (k_{12} + k_{13} + k_{10})\hat{A}_1 \\ s\hat{A}_2 - A_2(0) = k_{12}\hat{A}_1 - k_{21}\hat{A}_2 \\ s\hat{A}_3 - A_3(0) = k_{13}\hat{A}_1 - k_{31}\hat{A}_3 \end{cases} \tag{11}$$

Eq. set (11) can be rearranged into eq. set (12).

$$\begin{cases} -A_1(0) = \dfrac{r}{s} + k_{21}\hat{A}_2 + k_{31}\hat{A}_3 - (k_{12} + k_{13} + k_{10} + s)\hat{A}_1 \\ -A_2(0) = k_{12}\hat{A}_1 - (k_{21} + s)\hat{A}_2 \\ -A_3(0) = k_{13}\hat{A}_1 - (k_{31} + s)\hat{A}_3 \end{cases} \tag{12}$$

Eq. (3) can be expressed as $(K - sI_3)\cdot X = B$

$$\text{if } K = \begin{bmatrix} -(k_{12} + k_{13} + k_{10}) & k_{21} & k_{31} \\ k_{12} & -k_{21} & 0 \\ k_{13} & 0 & -k_{31} \end{bmatrix} \tag{13}$$

$$\text{and } X = \left[\hat{A}_1, \hat{A}_2, \hat{A}_3\right]^{\mathrm{T}}, B = \left[-\frac{r}{s} - A_1(0), -A_2(0), -A_3(0)\right]^{\mathrm{T}}. \tag{14),(15}$$

$$\text{Finally } \hat{A}_1 = \frac{D_1(\mathrm{s})}{|K - sI_3|} \text{ if } D_1(s) = \begin{vmatrix} -\dfrac{r}{s} - A_1(0) & k_{21} & k_{31} \\ -A_2(0) & -(k_{21} + s) & 0 \\ -A_3(0) & 0 & -(k_{31} + s) \end{vmatrix}. \tag{16}$$

$$\text{If } \begin{cases} a_0 = k_{10}k_{21}k_{31} \\ a_1 = k_{10}k_{31} + k_{10}k_{21} + k_{21}k_{31} + k_{21}k_{13} + k_{31}k_{12} \\ a_2 = k_{10} + k_{12} + k_{13} + k_{21} + k_{31} \end{cases} \tag{17}$$

$$\text{then } |K - sI_3| = -s^3 - a_2 s^2 - a_1 s - a_0 = -(s + \lambda_1)(s + \lambda_2)(s + \lambda_3). \tag{18}$$

The factorization applies Cardano's method, which is described in Appendix 2.

Appendix 2. Factorization of $|K - sI_3|$

According to Cardano's method, $s^3 + a_2 s^2 + a_1 s + a_0 = (s + \lambda_1)(s + \lambda_2)(s + \lambda_3)$

if $p = a_1 - \frac{a_2^2}{3}, q = \frac{2a_2^3}{27} - \frac{a_1 a_2}{3} + a_0, r_1 = \sqrt{-\frac{p^3}{27}}, \phi = \frac{\arccos\left(-\frac{q}{2r_1}\right)}{3}, r_2 = 2\sqrt[3]{r_1}$

then $\lambda_1 = \frac{a_2}{3} - \cos(\phi) r_2, \lambda_2 = \frac{a_2}{3} - \cos\left(\phi + \frac{2\pi}{3}\right) r_2, \lambda_3 = \frac{a_2}{3} - \cos\left(\phi + \frac{4\pi}{3}\right) r_2.$

The partial fraction expansion form of $\hat{A}_1$ is $\hat{A}_1 = \frac{w_0}{s} + \frac{w_1}{s + \lambda_1} + \frac{w_2}{s + \lambda_2} + \frac{w_3}{s + \lambda_3}$ (19)

and $w_0..w_3$ are infered in Appendix 3 and 4.

Appendix 3. Cp_{tb}: Cp **function following a bolus injection**

$Cp_{tb}(t)$ denotes the Cp function (an alias of c_1) following a single intravenous injection of dosage d at time tb. There is no drug being infused and there is no drug in all compartments so r, $A_2(0)$ and $A_3(0)$ are zero, $A_1(0)$ is d at time tb.

$$r = A_2(0) = A_3(0) = 0 \Rightarrow D_1(s) = -d(k_{21}+s)(k_{31}+s)$$

$$\frac{D_1(s)}{|K - sI3|} = \frac{-d(k_{21}+s)(k_{31}+s)}{-(s+\lambda_1)(s+\lambda_2)(s+\lambda_3)} = \frac{w_0}{s} + \frac{w_1}{s+\lambda_1} + \frac{w_2}{s+\lambda_2} + \frac{w_3}{s+\lambda_3} \Rightarrow w_0 = 0$$

$$\frac{d(k_{21}+s)(k_{31}+s)}{(s+\lambda_2)(s+\lambda_3)} = w_1 + \frac{w_2(s+\lambda_1)}{s+\lambda_2} + \frac{w_3(s+\lambda_1)}{s+\lambda_3}$$

$$\Rightarrow \begin{cases} w_1 = d \cdot \dfrac{(k_{21}-\lambda_1)(k_{31}-\lambda_1)}{(\lambda_2-\lambda_1)(\lambda_3-\lambda_1)} \\ w_2 = d \cdot \dfrac{(k_{21}-\lambda_2)(k_{31}-\lambda_2)}{(\lambda_3-\lambda_2)(\lambda_1-\lambda_2)} \\ w_3 = d \cdot \dfrac{(k_{21}-\lambda_3)(k_{31}-\lambda_3)}{(\lambda_1-\lambda_3)(\lambda_2-\lambda_3)} \end{cases} \tag{20}$$

Let $C_1 = \dfrac{(k_{21}-\lambda_1)(k_{31}-\lambda_1)}{(\lambda_1-\lambda_2)(\lambda_1-\lambda_3)V_1}, C_2 = \dfrac{(k_{21}-\lambda_2)(k_{31}-\lambda_2)}{(\lambda_2-\lambda_1)(\lambda_2-\lambda_3)V_1}, C_3 = \dfrac{(k_{21}-\lambda_3)(k_{31}-\lambda_3)}{(\lambda_3-\lambda_1)(\lambda_3-\lambda_2)V_1}$

then $Cp_{tb}(t) = \sum_{\sigma=1}^{3} d \cdot C_\sigma e^{-\lambda_\sigma (t-tb)}$. (21)

Appendix 4. $Cp_{tc\sim}$: *Cp* **function following the begining of an ongoing infusion**

$Cp_{tc\sim}(t)$ denotes the *Cp* function following an ongoing infusion that begins from time *tc* at rate *r*. There is no drug in all compartments before infusion so $A_1(0)$, $A_2(0)$ and $A_3(0)$ are zero.

$$A_1(0)=A_2(0)=A_3(0)=0 \Rightarrow D_1(s)=-\frac{r}{s}(k_{21}+s)(k_{31}+s) \tag{21}$$

$$\frac{D_1(s)}{|K-sI_3|}=\frac{-\frac{r}{s}(k_{21}+s)(k_{31}+s)}{-(s+\lambda_1)(s+\lambda_2)(s+\lambda_3)}=\frac{w_0}{s}+\frac{w_1}{s+\lambda_1}+\frac{w_2}{s+\lambda_2}+\frac{w_3}{s+\lambda_3} \tag{22}$$

$$\Rightarrow \frac{r(k_{21}+s)(k_{31}+s)}{(s+\lambda_1)(s+\lambda_2)(s+\lambda_3)}=w_0+s\left(\frac{w_1}{s+\lambda_1}+\frac{w_2}{s+\lambda_2}+\frac{w_3}{s+\lambda_3}\right) \tag{23}$$

$$\text{if } s=0 \text{ then } w_0=\frac{r\,k_{21}k_{31}}{\lambda_1\lambda_2\lambda_3}=\frac{r}{k_{10}} \tag{24}$$

$$\Rightarrow \frac{\frac{r}{s}(k_{21}+s)(k_{31}+s)}{(s+\lambda_2)(s+\lambda_3)}=w_1+(s+\lambda_1)\left(\frac{w_0}{s}+\frac{w_2}{s+\lambda_2}+\frac{w_3}{s+\lambda_3}\right) \tag{25}$$

$$\text{if } s=-\lambda_1 \text{ then } w_1=\frac{r}{\lambda_1}\cdot\frac{(k_{21}-\lambda_1)(k_{31}-\lambda_1)}{(\lambda_2-\lambda_1)(\lambda_3-\lambda_1)}=r\cdot\frac{C_1V_1}{\lambda_1} \tag{26}$$

$$\text{In the same way} \Rightarrow \begin{cases} w_2=\dfrac{r}{\lambda_2}\cdot\dfrac{(k_{21}-\lambda_2)(k_{31}-\lambda_2)}{(\lambda_3-\lambda_2)(\lambda_1-\lambda_2)}=r\cdot\dfrac{C_2V_2}{\lambda_2} \\ w_3=\dfrac{r}{\lambda_3}\cdot\dfrac{(k_{21}-\lambda_3)(k_{31}-\lambda_3)}{(\lambda_1-\lambda_3)(\lambda_2-\lambda_3)}=r\cdot\dfrac{C_3V_3}{\lambda_3} \end{cases} \tag{27),(28}$$

$$\therefore Cp_{tc\sim}(t)=-\sum_{\sigma=1}^{3} r\cdot\frac{C_\sigma}{\lambda_\sigma}e^{-\lambda_\sigma(t-tc)}+\frac{r}{V_1k_{10}} \tag{29}$$

Appendix 5. $Cp_{tc\sim td}$: *Cp* **function following the end of an infusion**

$Cp_{tc\sim td}$ denotes the *Cp* function following an infusion that begins from time *tc* and stopped at time *td*. Due to the linearity of eq. set (10), $Cp_{tc\sim td}$ is the function to subtract $Cp_{td\sim}(t)$ from $Cp_{tc\sim}(t)$.

$$
\begin{aligned}
&Cp_{tc\sim td}(t) = Cp_{tc\sim}(t) - Cp_{td\sim}(t) \\
&= \left(-\sum_{\sigma=1}^{3} r \cdot \frac{C_\sigma}{\lambda_\sigma} e^{-\lambda_\sigma (t-tc)} + \frac{r}{V_1 k_{10}} \right) - \left(-\sum_{\sigma=1}^{3} r \cdot \frac{C_\sigma}{\lambda_\sigma} e^{-\lambda_\sigma (t-td)} + \frac{r}{V_1 k_{10}} \right) \\
&= \sum_{\sigma=1}^{3} r \cdot \frac{C_\sigma}{\lambda_\sigma} \left(-e^{-\lambda_\sigma (t-tc)} + e^{-\lambda_\sigma (t-td)} \right)
\end{aligned}
\tag{30}
$$

Appendix 6. Cp_{ii}: Cp **trend following multiple infusions and injections**

d_i denotes the i-th injection dose, tb_i denotes the time to inject d_i and m denotes the length of bolus injection dose sequence (i=1 to m). r_j denotes the rate to which the j-th changing infusion rate, tf_j denotes the time to do the j-th rate-changing and n denotes the length of infusion rate sequence (j=1 to n). Cp_{ii} is the summation of these injection doses and infusion intervals.

$$Cp_{ii}(t) = \sum_{i=1}^{m} Cp_{tb_i} + \sum_{j=1}^{n-1} Cp_{tf_j \sim tf_{j+1}} + Cp_{tf_n \sim} = \sum_{i=1}^{m}\sum_{\sigma=1}^{3}\left(d_i \cdot C_\sigma e^{-\lambda_\sigma (t-tb_i)}\right)$$
$$+ \sum_{j=1}^{n-1}\sum_{\sigma=1}^{3} r_j \cdot \frac{C_\sigma}{\lambda_\sigma}\left(-e^{-\lambda_\sigma (t-tf_j)} + e^{-\lambda_\sigma (t-tf_{j+1})}\right) - \sum_{\sigma=1}^{3} r_n \cdot \frac{C_\sigma}{\lambda_\sigma} e^{-\lambda_\sigma (t-tf_n)} + \frac{r_n}{V_1 k_{10}} \quad (31)$$
$$= \sum_{\sigma=1}^{3} C_\sigma \left\{ \left(\sum_{i=1}^{m} d_i \cdot e^{\lambda_\sigma tb_i} \right) + \frac{1}{\lambda_\sigma} \left[\left(\sum_{j=1}^{n-1} r_j \cdot \left(-e^{\lambda_\sigma tf_j} + e^{\lambda_\sigma tf_{j+1}} \right) \right) - r_n \cdot e^{\lambda_\sigma tf_n} \right] \right\} \cdot e^{-\lambda_\sigma t} + \frac{r_n}{V_1 k_{10}}$$

$$\text{Let } r_0 = 0 \text{ and , for } \sigma = 1..3, \text{ and denote } F_\sigma = \left(\sum_{j=1}^{n-1} r_j \cdot \left(-e^{\lambda_\sigma tf_j} + e^{\lambda_\sigma tf_{j+1}} \right) \right) - r_n \cdot e^{\lambda_\sigma tf_n}$$
$$= r_0 \cdot e^{\lambda_\sigma tf_1} + r_1 \cdot \left(-e^{\lambda_\sigma tf_1} + e^{\lambda_\sigma tf_2} \right) + r_2 \cdot \left(-e^{\lambda_\sigma tf_2} + e^{\lambda_\sigma tf_3} \right) + \ldots \quad (32)$$
$$+ r_{n-1} \cdot \left(-e^{\lambda_\sigma tf_{n-1}} + e^{\lambda_\sigma tf_n} \right) - r_n \cdot e^{\lambda_\sigma tf_n} = \sum_{j=1}^{n} \left(r_{j-1} - r_j \right) e^{\lambda_\sigma tf_j}$$

$$\text{Let } \alpha_0 = \frac{r_n}{V_1 k_{10}} \text{ and denote } \begin{cases} B_\sigma = \sum_{i=1}^{m} d_i \cdot e^{\lambda_\sigma tb_i} \ (\sigma = 1..3) \\ \alpha_\sigma = C_\sigma \left(B_\sigma + \frac{F_\sigma}{\lambda_\sigma} \right) \end{cases} \quad (33),(34)$$

$$\Rightarrow Cp_{ii}(t) = \sum_{\sigma=1}^{3} C_\sigma \left(B_\sigma + \frac{F_\sigma}{\lambda_\sigma} \right) \cdot e^{-\lambda_\sigma t} + \frac{r_n}{V_1 k_{10}} = \alpha_0 + \sum_{\sigma=1}^{3} \alpha_\sigma e^{-\lambda_\sigma t}, \text{for } t \geq \max(tb_m, tf_n) \quad (35)$$

Appendix 7. Four-compartment mammillary model with an effect compartment

Let compartment 4 be the effect-site compartment and V_4 is supposed to be so small that the drug transported to and from V_4 is too small to affect A_1. That's the reason we can say that the *Cp* function is almost the same as the one in appendix 1-6 and k_{14} and k_{41} can be decided by the value of t_{peak} [2]. In addition to differential eq. set (10) is

$$\frac{dA_4}{dt} = k_{14}A_1 - k_{41}A_4 \tag{36}$$

Let *Ce* (drug concentration of effect compartment) be an alias of c_4. Apply the Laplace transform to eq. (36) yields:

$$s\hat{A}_4 - A_4(0) = k_{14}\hat{A}_1 - k_{41}\hat{A}_4 = k_{14}V_1\hat{C}p - k_{41}\hat{A}_4 \tag{37}$$

$$\because k_{14}V_1 = k_{41}V_4 \therefore \hat{A}_4 = V_4\hat{C}e = \frac{k_{14}V_1\hat{C}p + A_4(0)}{s + k_{41}} \tag{38}$$

$$\Rightarrow \hat{C}e = \frac{k_{41}\hat{C}p + \frac{A_4(0)}{V_4}}{s + k_{41}} \tag{39}$$

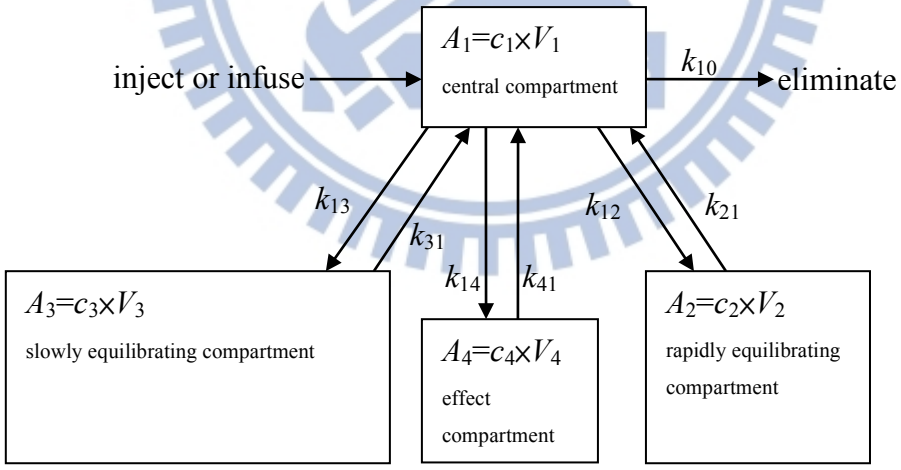

Figure 13. Four-compartment mammillary model with an effect compartment

Appendix 8. Ce_{tb}: Ce **function following a bolus injection**

$Ce_{tb}(t)$ denotes the Ce function correlated to $Cp_{tb}(t)$.

$$\because A_4(0)=0, Cp_{tb}=\sum_{\sigma=1}^{3} d\cdot C_\sigma e^{-\lambda_\sigma(t-tb)}$$

$$\Rightarrow \hat{C}e_{tb}=\frac{k_{41}}{s+k_{41}}\hat{C}p_{tb}=\sum_{\sigma=1}^{3} d\cdot C_\sigma \frac{k_{41}}{s+k_{41}}\frac{1}{s+\lambda_\sigma}$$

$$=\sum_{\sigma=1}^{3} d\cdot \frac{k_{41}C_\sigma}{k_{41}-\lambda_\sigma}\left(\frac{1}{(s+\lambda_\sigma)}-\frac{1}{(s+k_{41})}\right) \tag{40}$$

$$=\left(\sum_{\sigma=1}^{3} d\cdot \frac{k_{41}C_\sigma}{k_{41}-\lambda_\sigma}\frac{1}{(s+\lambda_\sigma)}\right)-\left(\sum_{\sigma=1}^{3} d\cdot \frac{k_{41}C_\sigma}{k_{41}-\lambda_\sigma}\frac{1}{(s+k_{41})}\right)$$

$$\text{Let}\ \lambda_4=k_{41}\ \text{then}\ Ce_{tb}(t)=\left(\sum_{\sigma=1}^{3} d\cdot \frac{k_{41}C_\sigma}{k_{41}-\lambda_\sigma}e^{-\lambda_\sigma(t-tb)}\right)-\left(d\cdot\sum_{\sigma=1}^{3}\frac{k_{41}C_\sigma}{k_{41}-\lambda_\sigma}\right)e^{-\lambda_4(t-tb)} \tag{41}$$

Appendix 9. $Ce_{tc\sim}$: *Ce* **function following the begining of an ongoing infusion**

$Ce_{tc\sim}(t)$ denotes the *Ce* function correlated to $Cp_{tc\sim}(t)$.

$$\because A_4(0)=0, Cp_{tc\sim}=-\sum_{\sigma=1}^{3} r\cdot\frac{C_\sigma}{\lambda_\sigma}e^{-\lambda_\sigma(t-t_c)}+\frac{r}{V_1k_{10}}$$

$$\Rightarrow \hat{C}e_{tc\sim}(t)=\frac{k_{41}}{s+k_{41}}\hat{C}p_{tc\sim}(t)=\frac{k_{41}}{s+k_{41}}\left(-\left(\sum_{\sigma=1}^{3} r\cdot\frac{C_\sigma}{\lambda_\sigma}\frac{1}{s+\lambda_\sigma}\right)+\frac{r}{V_1k_{10}}\frac{1}{s}\right)$$

$$=-\left(\sum_{\sigma=1}^{3} r\cdot\frac{k_{41}C_\sigma}{\lambda_\sigma}\frac{1}{(s+\lambda_\sigma)(s+k_{41})}\right)+\frac{r}{V_1k_{10}}\frac{k_{41}}{s(s+k_{41})} \quad (42)$$

$$=-\left(\sum_{\sigma=1}^{3} r\cdot\frac{k_{41}C_\sigma}{\lambda_\sigma(k_{41}-\lambda_\sigma)}\left(\frac{1}{s+\lambda_\sigma}-\frac{1}{s+k_{41}}\right)\right)+\frac{r}{V_1k_{10}}\left(\frac{1}{s}-\frac{1}{s+k_{41}}\right)$$

For $\sigma=1..3$, let $E_\sigma=\frac{k_{41}C_\sigma}{\lambda_\sigma(k_{41}-\lambda_\sigma)}$, and $E_4=\frac{1}{V_1k_{10}}-\sum_{\sigma=1}^{3}E_\sigma$

$$\hat{C}e_{tc\sim}(t)=-\left(\sum_{\sigma=1}^{3} r\cdot E_\sigma\left(\frac{1}{s+\lambda_\sigma}-\frac{1}{s+k_{41}}\right)\right)+\frac{r}{V_1k_{10}}\left(\frac{1}{s}-\frac{1}{s+k_{41}}\right)$$

$$=-\left(\sum_{\sigma=1}^{3} r\cdot E_\sigma\left(\frac{1}{s+\lambda_\sigma}\right)\right)-r\left(\frac{1}{V_1k_{10}}-\sum_{\sigma=1}^{3}E_\sigma\right)\frac{1}{s+k_{41}}+\left(\frac{r}{V_1k_{10}}\frac{1}{s}\right) \quad (43)$$

$$=-\left(\sum_{\sigma=1}^{4} r\cdot E_\sigma\left(\frac{1}{s+\lambda_\sigma}\right)\right)+\left(\frac{r}{V_1k_{10}}\frac{1}{s}\right)$$

$$\Rightarrow Ce_{tc\sim}(t)=-\sum_{\sigma=1}^{4} r\cdot E_\sigma e^{-\lambda_\sigma(t-tc)}+\frac{r}{V_1k_{10}} \quad (44)$$

Appendix 10. $Ce_{tc\sim td}$: ***Ce*** **function following the end of an infusion**

$Ce_{tc\sim td}$ denotes the *Ce* function correlated to $Cp_{tc\sim td}$. Due to the linearity $Ce_{tc\sim td}$ is the function to subtract $Ce_{td\sim}(t)$ from $Ce_{tc\sim}(t)$.

$$\begin{aligned}\therefore Ce_{tc\sim td} &== \left(-\sum_{\sigma=1}^{4} r\cdot E_\sigma e^{-\lambda_\sigma (t-tc)} + \frac{r}{V_1 k_{10}}\right) - \left(-\sum_{\sigma=1}^{4} r\cdot E_\sigma e^{-\lambda_\sigma (t-td)} + \frac{r}{V_1 k_{10}}\right) \\ &= \sum_{\sigma=1}^{4} r\cdot E_\sigma \left(-e^{-\lambda_\sigma (t-tc)} + e^{-\lambda_\sigma (t-td)}\right)\end{aligned} \tag{45}$$

Appendix 11. Ce_{ii}**:** Ce **trend function following multiple infusions and injections**

$Ce_{ii}(t)$ denotes the Ce function correlated to $Cp_{ii}(t)$.

$$Ce_{ii}(t) = \sum_{i=1}^{m} Ce_{tb_i} + \sum_{j=1}^{n-1} Ce_{tf_j \sim tf_{j+1}} + Ce_{tf_n \sim}$$

$$= \sum_{i=1}^{m} \left[\left(\sum_{\sigma=1}^{3} d_i \cdot \frac{k_{41} C_\sigma}{k_{41} - \lambda_\sigma} e^{-\lambda_\sigma (t - tb_i)} \right) - \left(d_i \cdot \sum_{\sigma=1}^{3} \frac{k_{41} C_\sigma}{k_{41} - \lambda_\sigma} \right) e^{-\lambda_4 (t - tb_i)} \right]$$

$$+ \sum_{j=1}^{n-1} \left[\sum_{\sigma=1}^{4} r_j \cdot E_\sigma \left(- e^{-\lambda_\sigma (t - tf_j)} + e^{-\lambda_\sigma (t - tf_{j+1})} \right) \right] - \sum_{\sigma=1}^{4} r_n \cdot E_\sigma e^{-\lambda_\sigma (t - tf_n)} + \frac{r_n}{V_1 k_{10}} \tag{46}$$

$$= \left[\sum_{\sigma=1}^{3} \frac{k_{41} C_\sigma}{k_{41} - \lambda_\sigma} \left(\sum_{i=1}^{m} d_i \cdot e^{\lambda_\sigma tb_i} \right) e^{-\lambda_\sigma t} \right] + \left(- \sum_{\sigma=1}^{3} \frac{k_{41} C_\sigma}{k_{41} - \lambda_\sigma} \right) \left(\sum_{i=1}^{m} d_i \cdot e^{\lambda_4 tb_i} \right) e^{-\lambda_4 t}$$

$$+ \sum_{\sigma=1}^{4} E_\sigma \left[\left(\sum_{j=1}^{n-1} r_j \cdot \left(- e^{\lambda_\sigma tf_j} + e^{\lambda_\sigma tf_{j+1}} \right) \right) - r_n \cdot e^{\lambda_\sigma tf_n} \right] e^{-\lambda_\sigma t} + \frac{r_n}{V_1 k_{10}}$$

$$\text{Let } F_4 = \left(\sum_{j=1}^{n-1} r_j \cdot \left(- e^{\lambda_4 tf_j} + e^{\lambda_4 tf_{j+1}} \right) \right) - r_n \cdot e^{\lambda_4 tf_n}$$

$$\Rightarrow Ce_{ii}(t) = \left[\sum_{\sigma=1}^{3} \frac{k_{41} C_\sigma B_\sigma}{k_{41} - \lambda_\sigma} e^{-\lambda_\sigma t} \right] - \left(\sum_{\sigma=1}^{3} \frac{k_{41} C_\sigma}{k_{41} - \lambda_\sigma} \right) \left(\sum_{i=1}^{m} d_i \cdot e^{\lambda_4 tb_i} \right) e^{-\lambda_4 t} + \sum_{\sigma=1}^{4} E_\sigma F_\sigma e^{-\lambda_\sigma t} + \frac{r_n}{V_1 k_{10}} \tag{47}$$

$$\text{Let } G_\sigma = \frac{k_{41} C_\sigma B_\sigma}{k_{41} - \lambda_\sigma} \text{ for } \sigma = 1 \sim 3, G_4 = - \left(\sum_{\sigma=1}^{3} \frac{k_{41} C_\sigma}{k_{41} - \lambda_\sigma} \right) \left(\sum_{i=1}^{m} d_i \cdot e^{\lambda_4 tb_i} \right)$$

$$\Rightarrow Ce_a = \left(\sum_{\sigma=1}^{3} G_\sigma e^{-\lambda_\sigma t} \right) + G_4 e^{-\lambda_4 t} + \sum_{\sigma=1}^{4} E_\sigma F_\sigma e^{-\lambda_\sigma t} + \frac{r_n}{V_1 k_{10}} \tag{48}$$

$$= \sum_{\sigma=1}^{4} (G_\sigma + E_\sigma F_\sigma) e^{-\lambda_\sigma t} + \frac{r_n}{V_1 k_{10}}$$

$$\text{Let } \varepsilon_0 = \frac{r_n}{V_1 k_{10}}, \text{and let } \varepsilon_\sigma = G_\sigma + E_\sigma F_\sigma \text{ for } \sigma = 1 \text{ to } 4. \Rightarrow Ce_{ii} = \varepsilon_0 + \sum_{\sigma=0}^{4} \varepsilon_\sigma e^{-\lambda_\sigma t} \tag{49}$$

Appendix 12. How to find all of the roots of a multi-exponential function by real root isolation method?

Function f is a *n* degree multi-exponential function (MEF), denoted by Degree(*f*)=*n*, if $f = a_0 + \sum_{i=1}^{n} a_i e^{b_i x}, \prod_{i=1}^{n} a_i b_i \neq 0 \wedge b_i \neq b_j$ for $i \neq j$. For any MEF f:S=$[a,b]$→R, denote R_S^f as the set of the roots of $f(t)$=0. Theorem 1 proves R_S^f is a finite set if $R_S^{\frac{d}{dt}f}$ is finite. Theorem 2 proves the size of R_S^f is no more than the Degree(*f*).

Theorem 1. $\left|R_S^f\right| \leq \left|R_S^{\frac{d}{dt}f}\right| + 1$

Let $S = [a,b]$ and f:S→R is a smooth function. Let $R_S^f = \{x | f(x) = 0 \wedge x \in S\}$.

If the size of $R_S^{\frac{d}{dt}f}$ is finite and $R_S^{\frac{d}{dt}f} \cup \{a,b\} = \{r_0, r_1, ... r_{m+1}\}$

r_i is a root of $R_S^{\frac{d}{dt}f}$, $r_0 = a, r_{m+1} = b, r_i < r_{i+1}$ for i=0,1...m then

$(a).f$ is strictly monotonic in $[r_i, r_{i+1}], i = 0..m$
$(b).f(r_i)f(r_{i+1}) \leq 0 \Rightarrow \exists! x \in [r_i, r_{i+1}]: f(x) = 0$
$(c).f(r_i)f(r_{i+1}) > 0 \Rightarrow \forall x \in [r_i, r_{i+1}]: f(x) \neq 0$.
$(d).\left|R_S^f\right| \leq \left|R_S^{\frac{d}{dt}f}\right| + 1$

proof:

(a). $R_{(r_i, r_{i+1})}^{\frac{d}{dt}f} = \phi$ otherwise $\frac{d}{dt}f$ has a root not belong to $R_S^{\frac{d}{dt}f}$. If f is not strictly monotonic, there must be an x_3: $x_1<x_3<x_5$ makes 1. $f(x_1) \leq f(x_3)$ and $f(x_3) \geq f(x_5)$ or 2. $f(x_1) \geq f(x_3)$ and $f(x_3) \leq f(x_5)$.

Consider case 1 first, and case 2 is similar. Since f is differenciable, there must be an x_2, $x_1<x_2<x_3$,makes $\frac{d}{dt}f(x_2) = \frac{f(x_3) - f(x_1)}{x_3 - x_1}$ by mean value theorem, so $\frac{d}{dt}f(x_2) \geq 0$.

For the same reason, $\exists x_4, x_3 < x_4 < x_5 \ni \frac{d}{dt}f(x_4) \leq 0$. Since $\frac{d}{dt}f$ is continuous

$\exists x_6, x_2 < x_6 < x_4 \ni \frac{d}{dt}f(x_6) = 0$ by intermediate value theorem. This contradict with

$R^{\frac{d}{dt}f}_{(r_i,r_{i+1})} = \phi$. For the same reason, case 2 would not stand. So, f is strictly monotonic in $[r_i,r_{i+1}]$.

(*b*). f has a root in $[r_i,r_{i+1}]$ because 1. if $f(r_i)f(r_{i+1}) < 0 \Rightarrow \exists x, r_i < x < r_{i+1} \ni f(x) = 0$ by intermediate value theorem 2. if $f(r_i)f(r_{i+1}) = 0 \Rightarrow \exists x \in \{r_i, r_{i+1}\} \ni f(x) = 0$. Since f is strictly monotonic in $[r_i,r_{i+1}]$, there must be only one root in $[r_i,r_{i+1}]$.

(*c*). If $f(r_i)f(r_{i+1}) > 0 \wedge \exists x \in [r_i, r_{i+1}]: f(x) = 0$ then f can not be monotonic, this contradict with (*a*).

(*d*). $\because S = \bigcup_{i=0}^{m}[r_i, r_{i+1}] \Rightarrow |R_S^f| \le \sum_{i=0}^{m} |R^f_{[r_i,r_{i+1}]}| \le m+1 = \left|R_S^{\frac{d}{dt}f}\right| + 1$

Theorem 2. If f is a MEF, then $|R_S^f| \le Degree(f)$.

proof:

(a) If $Degree(f)$=1,that is $f = a_0 + a_1 e^{b_1 x}$ and $a_1 b_1 \neq 0$.

If $-\frac{a_0}{a_1} > 0 \wedge \frac{\ln(-a_0/a_1)}{b_1} \in S$,then $R_S^f = \{\frac{\ln(-a_0/a_1)}{b_1}\}$ otherwise $R_S^f = \phi$. $\Rightarrow |R_S^f| \le 1$

(b) 1. If $\forall f : Degree(f) = n-1 \ge |R_S^f|$ stand.

2. For all f:Degree(f)=n, $\frac{d}{dt} f = \sum_{i=1}^{n} a_i b_i e^{b_i x} = e^{b_n x}\left(a_n b_n + \sum_{i=1}^{n-1} a_i b_i e^{(b_i - b_n)x}\right)$.

3. Let $f^* = a_n b_n + \sum_{i=1}^{n-1} a_i b_i e^{(b_i - b_n)x} \Rightarrow |R_S^{f^*}| \le n-1 \because Degree(f^*) \le n-1$.

4. $\forall x \in S : e^{b_n x} \neq 0 \Rightarrow R_S^{\frac{d}{dt}f} = R_S^{f^*}$.

5. $|R_S^f| \le \left|R_S^{\frac{d}{dt}f}\right| + 1$ (by Theorem 1)

$= |R_S^{f^*}| + 1 \le n \Rightarrow |R_S^f| \le n$

(c) According to the principle of induction, it is proved.

According to Theorem 2, an n-degree MEF f has at most n roots, and if the roots of $\frac{d}{dt} f$ is available, every root of f can be approached with bisectional method in the interval between two adjacent points of roots or end points of domain S. The root set of $\frac{d}{dt} f$ is identical to the one of f^* which is a MEF of lower degree. Repeat this procedure until the problem is

transformed to finding the root of an exponential function. According to Theorem 2, the root set of an exponential function is finite, so the root set of the serial of f^* and f are finite.

Appendix 13. The algorithms to find all of the real roots of a multi-exponential function by real root isolation method

GetRootSet(f,S) // $S=\{a,b\}$: the set of end points of the domain of f

// $f = a_0 + \sum_{i=1}^{n} a_i e^{b_i t}, n \in \mathbf{N}$, Degree($f$)=$n$

1 **if** n=1
2 **then**
3 **if** $a_0 \cdot a_1 < 0$
4 **then** **return** $\{\frac{\ln(-a_0/a_1)}{b_1}\}$
5 **else** **return** ϕ
6 **else** // n>1
7 $E \leftarrow$ GetExtremumSet(f,S) // E: the set of the extremum of f

/* $E \in R_S^{\frac{d}{dt}f} \cup \{a,b\} = \{r_0, r_1, .. r_{m+1}\}$ because f is smooth. According to theorem 1.(a) f is strictly monotonic in every [ri,ri+1] so it is strictly montonic in the interval between two adjacent element of E. */

8 $R \leftarrow \phi$ // R: the set of the roots of f
9 **if** $f(a)=0$ **then** $R \leftarrow R \cup \{a\}$ // a: the left end of the domain of f
10 **for** $i \leftarrow 1$ **to** $|E|-1$ // find all of the roots of f(Theorem 1.b,1.c)
11 **do** **if** $f(E[i]) \cdot f(E[i+1]) \le 0$ // When $f(E[i]) \cdot f(E[i+1])>0$ there is no root between in [$E[i]$, $E[i+1]$] (Theorem 1.c). When $f(E[i]) \cdot f(E[i+1]) \le 0$ there is exactly one root in that interval (Theorem 1.b).
12 **then**
13 $r \leftarrow$bisectionally approach the root located in the interval [$E[i]$,$E[i+1]$] // the bisection method is called no more than n times
14 $R \leftarrow R \cup \{r\}$
15 **if** $f(b)=0$ **then** $R \leftarrow R \cup \{b\}$ // b: the right end of the domain of f
16 **return** R

GetExtremumSet(f,S) // $S=\{a,b\}$: the set of end points of the domain of f
1 $E \leftarrow S$ // E: the set of the extremum of f
2 **if** Degree(f)>1
3 **then** calculate f^* // $f^* = a_n b_n + \sum_{i=1}^{n-1} a_i b_i e^{(b_i - b_n)t}$
4 $R' \leftarrow$GetRootSet(f^*,S)
5 $E \leftarrow$select extrema of f from $R' \cup S$
6 **return** E

A multi-exponential function (MEF) has the number of roots no more than its degree. If

the number of sampling points in the time domain of a MEF is n_{sp} then to solve a root with bisection method need to calculate the value of MEF as many times as $O(\lg n_{sp})$.To calculate the value of a MEF need to call exponentail function as many times as the degree of it. If the degree of f, f^*, $(f^*)^*$ ... are n, n-1, n-2 ... then exponential function is called for $n \cdot O(\lg n_{sp}) \cdot n + (n\text{-}1) \cdot O(\lg n_{sp}) \cdot (n\text{-}1) + (n\text{-}2) \cdot O(\lg n_{sp}) \cdot (n\text{-}2) + \ldots = O(n^3 \lg n_{sp})$ times. For *Ce* trend, n is a small integer (=4), so the time it takes to find the roots of a MEF is $O(\lg n_{sp})$.

Appendix 14. Inject more drug produces higher *TMax*.

Suppose we are searching for an optimal injection dose at time t_0 after a serial of maual injections and/or changes of infusion rate. It consumes time to do linear search for all possible injection dose and find out the least dose which can drive the maximum of *Ce* trend (*TMax*) close to and no more than the upper bound of *Cet* range (*UB*).

Let *Pu* be the peak value after the injection of one unit dose to an object without any drug in its body and *Qd* be the step quantity of injection dose. Due to the linearity of the system, any injection dose larger than *UB*/*Pu* must drive *Ce* to the level higher than *UB*. So the injection dose is limited in the range of [0,*UB*/*Pu*], and steps by *Qd* from 0. Denote *k* as the number of all possible dose and

$$k = \left\lfloor \frac{UB}{Pu \cdot Qs} \right\rfloor + 1. \tag{50}$$

It takes the time of $O(k)$ to do a linear search. If *TMax* is correlated with the dose injected (*d*) at t_0, the value of optimal injection dose can be appoached by bisection method in $O(\lg k)$ time.

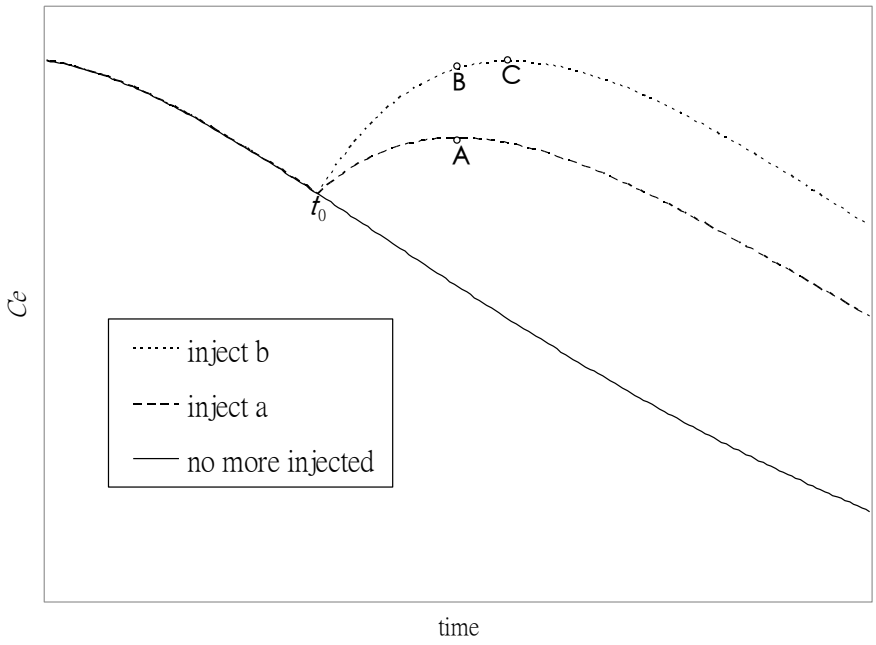

Figure 14. Larger injection doses produce higher *TMax*. If point **A** is the highest point of *Ce* trend following injecting dose ***a*** at time t_0 and point **C** is the highest point of *Ce* trend following injecting dose ***b*** at time t_0. then **C** is always higher than **A**. Let **B** be a point on *Ce* trend of dose ***b*** at the time of point **A**. **B** is higher than **A** for ***a***<***b*** and the linearity of pharmacokinetic model. **C** is higher than **B** because **C** is the maximum of dose ***a***.

Theorem 3. The maximum of the trend (*TMax*) following t_0 is correlated with the dose d injected at t_0.

proof: The yellow line in figure 14 is the *Ce* trend produced by the administration history before t_0. If t_0 is the time to calculate an optimal dose, the pink and blue lines are the *Ce* trend following two different dose ***a*** and ***b*** and ***a***<***b.*** Let point A and C denote the time and maximal values following dose ***a*** and ***b*** separately. Let point B be the point on the blue line at the time of point A. The *Ce* value of point C is always higher than point A because firstly, the *Ce* value of point B is higher than that of point A due to the linearity of the system. Secondly, the *Ce* value of point C is equal to or higher than that of point B because point C is the maximum of the blue line. In other words: if ***a***<***b*** then *TMax*(***a***)<*TMax*(***b***). So the value of optimal injection dose can be searched by bisection method.

Appendix 15. Infuse drug faster produces higher *TMin*.

Suppose we are searching for an optimal infusion rate at time t_0 after a serial of manual administrations. Optimal infusion rate is the minimal rate that produces the minimum of *Ce* trend (*TMin*) close to and no less than the lower bound of *Cet* range (*LB*). To do linear search from all possible infusion rate is time-consuming.

We choose the upper limit of infusion rate as 999.9 ml/hr which is higher than most of the specification of clinical infusion pumps. Let *Qr* be the step quantity of infusion rate and denote *k* as the number of all possible infusion rate and

$$k = \lfloor 999.9/Qr \rfloor + 1. \tag{51}$$

It takes the time of $O(k)$ to do a linear search. If *TMin* is correlated with the infution rate(r) at t_0, the value of optimal infusion rate can be found by bisection method in $O(\lg k)$ time.

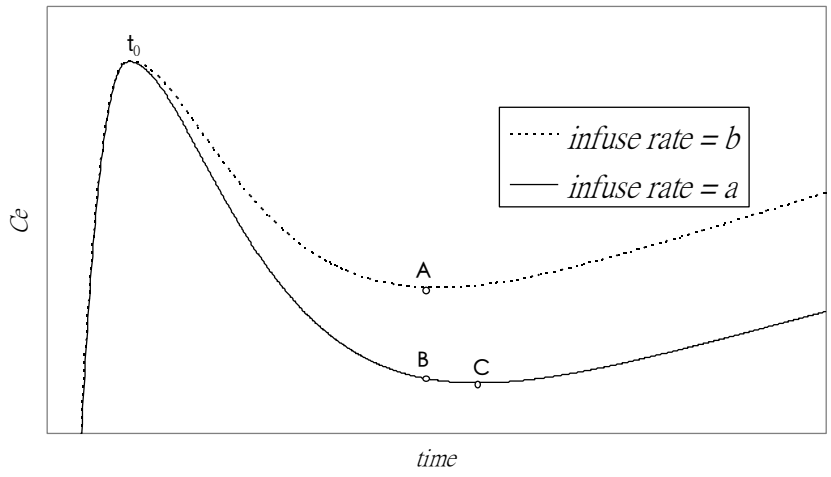

Figure 15. Faster infusion rates produce higher *TMin.* If point **A** is the lowest point of *Ce* trend following the rate ***a*** infusion begining at time t_0 and point **C** is the lowest point of *Ce* trend following the rate **b** infusion begining at time t_0. Then **C** is lower than **A.** Let **B** be a point on *Ce* trend of rate ***b*** at the time of point **A**. **B** is lower than **A** for ***a***>***b*** and the linearity of pharmacokinetic model. **C** is lower than **B** because **C** is the minimum of rate ***a***.

Theorem 4. The minimum of the trend (*TMin*) following t_0 is correlated with *r*.

proof: The yellow and pink lines are the trend of *Ce* produced by the same history of manual administrations before t_0 but the infusion rates are changed to ***a*** or ***b*** separately and ***a***<***b***. Let point A and C denote the time and minimal values following t_0 on the two lines. Let point B be the point on the yellow line at the time of Point A. The *Ce* value of point C is

always higher than point A because firstly, the *Ce* value of point A is always higher than point B due to the linearity of the system. Secondly, the *Ce* value of point B is equal to or higher than that of point C because point C is the minimum of the yellow line. In other words: if $\boldsymbol{a}<\boldsymbol{b}$ then $TMin(\boldsymbol{a})<TMin(\boldsymbol{b})$. So the optimal infusion rate can be searched by bisection method.

Appendix 16. The first order difference equations used in numerical linear search method

Using Euler's numerical technique, we can convert eq. set (10) to first-order difference equations [2]. In other words, we convert from a continuous time frame, where Time= *t*, to a discrete time frame, where $t = n\Delta t$. The first order difference equations, at Time *t*, are thus

$$\begin{cases} \Delta A_1(t) = d + \left(A_2(t)k_{21} + A_3(t)k_{31} + A_4(t)k_{41} - A_1(t)(k_{10} + k_{12} + k_{13} + k_{14}) + r\right)\Delta t \\ \Delta A_2(t) = \left(A_1(t)k_{12} - A_2(t)k_{21}\right)\Delta t \\ \Delta A_3(t) = \left(A_1(t)k_{13} - A_3(t)k_{31}\right)\Delta t \\ \Delta A_4(t) = \left(A_1(t)k_{14} - A_4(t)k_{41}\right)\Delta t \end{cases} \quad (52)$$

Appendix 17. The algorithm of analytical linear search method (ALS)

GetExtremumSetByALS()

1 $c \leftarrow Ce(t_0)$ // c is current Ce value,t_0 is the current time
2 $E \leftarrow \{(t_0, c)\}$ // include the time-Ce pair of the time on the left border of time domain
3 $n \leftarrow Ce(t_0+1)$ // n is the Ce value of the next second
4 $s \leftarrow$ SignOf(n - c) // s is the sign of the next second Ce minus the current Ce
5 **for** $t \leftarrow t_0+1$ **to** t_0+z-1 // t_0+z is the right border of the time domain. z denotes the size of time domain
6 $c \leftarrow n$ // $c \leftarrow Ce(t)$
7 $n \leftarrow Ce(t+1)$
8 $r \leftarrow s$ // r is the sign of $Ce(t)$ - $Ce(t\text{-}1)$
9 $s \leftarrow$ SignOf(n - c) // s is the sign of $Ce(t+1)$ - $Ce(t)$
10 **if** $s \neq r$ // if the sign is changing
11 **then** $E \leftarrow E \cup \{(t, c)\}$ // then include the time-Ce pair on time t
12 $E \leftarrow E \cup \{(t_0 + TDS, n)\}$ // include the right border of time domain
13 Remove the points that are neither local maximum nor local minimum from E.
14 **return** E

Appendix 18. The algorithm of numerical linear search method (NLS)

```
GetExtremumSetByNLS()
1   for i=1 to 4 do
2       A_i ← current drug mass of compartment i // maintained by system
3   c ← A_4/V_4                          // c is current Ce value
4   E ← {(t_0, c)}                       // include the time-Ce pair of the time on the left border of time domain
5   Calculate ΔA_1 ~ ΔA_4                // see [appendix 16]
6   for i=1 to 4 do A_i ← A_i+ΔA_i
7   n ← A_4/V_4                          // n is the Ce value of the next second
8   s = SignOf(n - c)                    // s is the sign of the next second Ce minus the current Ce
9   for t ← t_0+1 to t_0+z – 1           // t_0+z is the right border of the time domain. z denotes the size of time domain
10      c ← n                            // c ←Ce(t)
11      Calculate ΔA_1 ~ ΔA_4            // [appendix 16]
12      for i=1 to 4 do A_i ← A_i+ΔA_i
13      n ← A_4/V_4                      // n ← Ce(t+1)
14      r ← s                            // r is the sign of Ce(t) - Ce(t-1)
15      s ← SignOf(n-c)                  // s is the sign of Ce(t+1) - Ce(t)
16      if      s ≠ r                    // if the sign is changing
17      then    E ← E ∪ {(t, c)}         // then include the time-Ce pair on time t
18  E ← E ∪ {(t_0 + TDS, n)}             // include the right border of time domain
19  Remove the points that are neither local maximum nor local minimum from E.
20  return E
```

Autobiography

簡　　歷

我出生於新竹縣新埔鎮(1966)，並家鄉就學直到國中階段。在高中入學前參加交大暑期計算機研習營接觸到計算機(CDC Cyber)學習工程與商用語言(FORTRAN & COBOL)，而對資訊科學產生興趣(1981)。

在建國中學開始在電腦教室使用個人電腦(Apple II)，首次探索程式撰寫的領域，體會軟體開發的無限寬廣的可能與挑戰，與引人入勝的成就感。大學考取陽明醫學系(1985)，大一就參與電腦社的創立，也有機會在計算機中心打工。在當時的中心主任指導之下才略為了解計算機理論與演算法的基礎概念。

畢業後於省立桃園醫院完成麻醉科住院醫師訓練(1997)，而後擔任麻醉科主治醫師，歷任於省立竹東醫院(1997)，彰化基督教醫院(1999)與台中中港澄清醫院(2009)。基於對資訊技術的興趣，在執業期間仍不間斷的自修相關知識，醫院長官也常委以資訊相關的醫療或管理業務。

由於深感麻醉學的發展或醫院管理需要結合資訊科學的理論與資訊工程的設計實做與驗證，並有感於自身學識的不足，故投考交通大學資工所在職專班(2007)。求學的目的除了求充實學養與自我實現，主要是想發展跨領域的研究，好將資訊科學與科技應用在麻醉學的基礎、應用與管理方面。尤其我的興趣在於麻醉藥物的動力學控制方面，入學之後總希望能多研習各種控制理論與人工智慧的學門。

在職專班的同學幾乎都是資訊與電子相關行業的工程師，相對於多數出身於科班本系的同學而言，許多課程對我而言陌生又艱澀。尤其每週駕駛高速公路通車六百公里，而醫院的工作、值班絲毫未減，加上家庭責任正是最為人生中沉重的時期，又面臨家中尊親病故，孩子學習障礙種種問題，曾幾度有難以為繼，幾乎放棄的想法。

幸好交通大學資工系的老師都懷抱教學熱誠，總能不煩不倦的解答我的疑惑。尤其是我的指導老師蕭子健教授更是在我的修業過程中給我極大的鼓勵與支持。蕭老師細心耐心的指導，正是學生的福氣，特別是像我這樣工作多年重新求學的學生，更是心懷感恩點滴在心頭。總算天道酬勤，在努力的加強自我的不足之處，學習的成績竟還不差，曾獲書卷獎，感覺頗受鼓勵。

畢業在即，回首在交通大學的求學經歷，不僅是此時此期的收穫，希望這段不凡的經歷也成為往後人生階段的金鑰，開啟通往驚異之旅的門窗。